Polarized forward-backward asymmetries of lepton pair in $B \to K_1 \ell^+ \ell^-$ decay in the presence of New physics

Faisal Munir*[1], Saadi Ishaq†[1,3], Ishtiaq Ahmed‡[2,4]
[1] *Center for Future High Energy Physics, Institute of High Energy Physics, Chinese Academy of Sciences, Beijing 100049, China*
[2] *National Centre for Physics, Quaid-i-Azam University Campus, Islamabad, 45320 Pakistan*
[3] *Department of Physics, University of Gujrat, Hafiz Hayat Campus, Gujrat, Pakistan*
[4] *Laboratòrio de Fsica Teòrica e Computacional, Universidade Cruzeiro do Sul, 01506-000 São Paulo, Brazil*

(Dated: November 24, 2015)

Double polarized forward-backward asymmetries in $B \to K_1(1270, 1400)\ell^+\ell^-$ with $\ell = \mu, \tau$ decays are studied, using most general non-standard local four-fermi interactions, where the mass eigenstates $K_1(1270)$ and $K_1(1400)$ are the mixture of $^1P_1$ and $^3P_1$ states with the mixing angle θ_K. We have calculated the expressions of nine doubly polarized forward-backward asymmetries and it is presented that the polarized lepton pair forward-backward asymmetries are greatly influenced by the new physics. Therefore, these asymmetries are interesting tool to explore the status of new physics in near future, specially at LHC.

I. INTRODUCTION

Rare B decays mediated through the flavor changing neutral current (FCNC) $b \to s(d)\ell^+\ell^-$ transitions not only provide a testing ground for the gauge structure of standard model (SM) but are also an effective way to look for the physics beyond the SM. As we know that in SM the Wilson coefficients C_7, C_9 and C_{10} of the operators O_7, O_9 and O_{10} at $\mu = m_b$ are used to describe the $b \to s\ell^+\ell^-$ transition. Therefore, in these transitions, NP effects can be incorporated in two different ways: one is through new contributions to Wilson coefficients and the other is via the introduction of new operators in effective Hamiltonian which are absent in the SM.

Though the decay distribution of inclusive decays such as $B \to X_{s,d}\ell^+\ell^-$ is theoretically better understood but hard to be measured experimentally. In opposite, the exclusive decays such as $B \to (K, K^*, K_1, \rho)\ell^+\ell^-$ are easy to detect experimentally but are tough to calculate theoretically as the difficulty lies in describing the hadronic structure, which are the main source of uncertainties in the predictions of exclusive rare decays.

The exploration of physics beyond the SM through various inclusive B meson decays such as $B \to X_{s,d}\ell^+\ell^-$ and their corresponding exclusive processes, $B \to M\ell^+\ell^-$ with $M = K, K^*, K_1, \rho$ etc., have already been studied [1–5]. These studies showed that the above mentioned inclusive and exclusive decays of B meson are very sensitive to the flavor structure of the SM and provide an effective way to explore NP effects.

Regarding this precise measurements of different experimental observables for $b \to s\ell^+\ell^-$ decay such as branching ratio, forward-backward asymmetry, various polarization asymmetries of the final state leptons, etc could be useful in establishing the status of new physics (NP) in near future, specially at LHC. For this reason, many exclusive B meson processes based on $b \to s\,(d)\,\ell^+\ell^-$ such as $B \to K\,(K^*)\,\ell^+\ell^-$[6–12], $B \to \phi\ell^+\ell^-$[13], $B \to \gamma\ell^+\ell^-$[14–16] and $B \to \ell^+\ell^-$[17] have already been studied.

It has been mentioned in [18] that measurement of many additional observables, would be possible by studying the simultaneous polarizations of both leptons in the final state, which in turn would be useful in testing the SM and highlighting new physics beyond the SM. It should be mentioned here that double lepton polariztion asymmetries in $B \to K^*\tau^+\tau^-$[19], $B \to K\ell^+\ell^-$[20], $B \to \rho\ell^+\ell^-$[21] and $B \to K_1\ell^+\ell^-$[22, 23] have already been studied. Along with other observables, forward backward asymmetry is also an efficient observable to explore NP beyond the SM. In this regard, double lepton polarization forward-backward asymmertries in $B \to K^*\ell^+\ell^-$[24, 25], $B \to K\ell^+\ell^-$[26], $B \to \rho\ell^+\ell^-$[27] and in $B_s \to \gamma\ell^+\ell^-$[28] have already been explored. We would like to emphasise here that the situation which makes $B \to K_1\ell^+\ell^-$ decay more interesting than $B \to K^*\ell^+\ell^-$ is the mixing of axial vector states K_{1A} and K_{1B} which are the $^3P_1$ and $^1P_1$ states respectively. Therefore, it is also interesting to see that how polarized forward-backward asymmetries of $B \to K_1\ell^+\ell^-$ are influenced in the presence of new physics. So in the present work polarized forward-backward asymmetry in the exclusive decay $B \to K_1\ell^+\ell^-$ are addressed using most general

* faisalmunir@ihep.ac.cn
† Saadi.ishaq@uog.edu.pk
‡ ishtiaq@ncp.edu.pk

effective Hamiltonian, including all forms of possible interactions, similar to the case of $B \to K^* \ell^+ \ell^-$[24] decay. The physical states $K_1(1270)$ and $K_1(1400)$ are superposition of the P-wave states in the following way

$$|K_1(1270)\rangle = |K_{1A}\rangle \sin\theta_K + |K_{1B}\rangle \cos\theta_K \quad (1)$$
$$|K_1(1400)\rangle = |K_{1A}\rangle \cos\theta_K - |K_{1B}\rangle \sin\theta_K \quad (2)$$

If we define, $y = \sin\theta_K$ then above Eqs. become

$$|K_1(1270)\rangle = |K_{1A}\rangle y + |K_{1B}\rangle \sqrt{1-y^2}$$
$$|K_1(1400)\rangle = |K_{1A}\rangle \sqrt{1-y^2} - |K_{1B}\rangle y$$

where the magnitude of the mixing angle θ_K has been estimated [29] to be $34^\circ \leq |\theta_K| \leq 58^\circ$ and the study of $B \to K_1(1270)\gamma$ impose the limit [30] on the mixing angle as

$$\theta_K = -(34 \pm 13)^\circ \quad (3)$$

where minus sign of θ_K is related to the chosen phase of K_{1A} and K_{1B} [30].

The manuscript is presented as follows. In sec. II, we devise our required theoretical framework which is followed by two Subsections. II A and II B, relating to mixing of $K_1(1270)$ and $K_1(1400)$, form factors and constraints on the coefficients of NP operators used in this study. Sec. III, is devoted to analytical calculations and the explicit expressions of doubly polarized forward-backward asymmetries. In Sec. IV, we give the numerical analysis with discussion about the observables underconsiderations. We end our work by giving concluding remarks in Sec. V.

II. THEORETICAL FORMALISM

At the quark level $B \to K_1(1270, 1400)\ell^+\ell^-$ decays are induced by the transition $b \to s\ell^+\ell^-$, which in the SM, is described by the following effective Hamiltonian [31]

$$\mathcal{H}_{eff}^{SM}(b \to s\ell^+\ell^-) = -\frac{G_F \alpha}{\sqrt{2}\pi} V_{tb} V_{ts}^* \Big\{ C_9^{effSM} (\bar{s}\gamma_\mu L b)(\bar{\ell}\gamma^\mu \ell)$$
$$+ C_{10}(\bar{s}\gamma_\mu L b)(\bar{\ell}\gamma^\mu \gamma_5 \ell) - 2m_b C_7^{effSM} (\bar{s} i\sigma_{\mu\nu} \frac{q^\nu}{q^2} R b)(\bar{\ell}\gamma^\mu \ell) \Big\} \quad (4)$$

where $R, L = (1 \pm \gamma_5)/2$ are the projector operators and q^2 is the square of momentum transfer while $C's$ are Wilson coefficients. The effective Wilson coefficient $C_9^{effSM}(\mu)$, can be decomposed into the following three parts [3, 5]

$$C_9^{effSM}(\mu) = C_9(\mu) + Y_{SD}(z, \hat{s}) + Y_{LD}(z, \hat{s}),$$

where the parameters z and $\hat{s}$ are defined as $z = m_c/m_b$, $\hat{s} = q^2/m_b^2$. It is important to mention here that in our numerical calculations of asymmetries and their average values, we do not include $Y_{LD}(z, \hat{s})$, otherwise the asymmetries would be largely effected by the contributions of J/ψ and $\psi(2s)$ resonance around $s = 10GeV^2$ and $s = 14GeV^2$ respectively. The explicit expressions for short-distance contributions $Y_{SD}(z, \hat{s})$ and long distance contributions $Y_{LD}(z, \hat{s})$ are given in [3, 5].

New physics effects are explored for $B \to K_1 l^+ l^-$ channel by considering the most general local four-fermi interactions. In this regard the total effective Hamiltonian is given by

$$\mathcal{H}_{eff} = \mathcal{H}_{eff}^{SM} + \mathcal{H}_{eff}^{VA} + \mathcal{H}_{eff}^{SP} + \mathcal{H}_{eff}^{T} \quad (5)$$

where

$$\begin{aligned}
\mathcal{H}_{eff}^{VA} &= \frac{G_F\alpha}{\sqrt{2}\pi}V_{ts}^*V_{tb}\Big\{C_{LL}\bar{s}_L\gamma^\mu b_L\bar{l}_L\gamma^\mu l_L \\
&+ C_{LR}\bar{s}_L\gamma^\mu b_L\bar{l}_R\gamma^\mu l_R + C_{RL}\bar{s}_R\gamma^\mu b_R\bar{l}_L\gamma^\mu l_L \\
&+ C_{RR}\bar{s}_R\gamma^\mu b_R\bar{l}_R\gamma^\mu l_R\Big\} \\
\mathcal{H}_{eff}^{SP} &= \frac{G_F\alpha}{\sqrt{2}\pi}V_{ts}^*V_{tb}\Big\{C_{LRLR}\bar{s}_L b_R\bar{l}_L l_R + C_{RLLR}\bar{s}_R b_L\bar{l}_L l_R \\
&+ C_{LRRL}\bar{s}_L b_R\bar{l}_R l_L + C_{RLRL}\bar{s}_R b_L\bar{l}_R l_L\Big\} \\
\mathcal{H}_{eff}^{T} &= \frac{G_F\alpha}{\sqrt{2}\pi}V_{ts}^*V_{tb}\Big\{C_T\bar{s}\sigma_{\mu\nu}b\bar{l}\sigma^{\mu\nu}l \\
&+ iC_{TE}\epsilon_{\mu\nu\alpha\beta}\bar{l}\sigma^{\mu\nu}l\bar{s}\sigma^{\alpha\beta}b\Big\} \qquad (6)
\end{aligned}$$

while $\mathcal{H}_{eff}^{SM}$ is given in Eq. (4) and C_X are the coefficients of the four-Fermi interactions. Defining the combinations

$$\begin{aligned}
R_V &= \frac{1}{2}(C_{LL}+C_{LR}), \quad R_A = \frac{1}{2}(C_{LR}+C_{LL}) \\
R'_V &= \frac{1}{2}(C_{RR}+C_{RL}), \quad R'_A = \frac{1}{2}(C_{RR}-C_{RL}) \\
R_S &= \frac{1}{2}(C_{LRRL}+C_{LRLR}), \quad R_P = \frac{1}{2}(C_{LRLR}-C_{LRRL}) \\
R'_S &= \frac{1}{2}(C_{RLRL}+C_{RLLR}), \quad R'_P = \frac{1}{2}(C_{RLLR}-C_{RLRL})
\end{aligned}$$

where $R_A, R_V, R'_A, R'_V, R_S, R_P, R'_S, R'_P, C_T$ and C_{TE} represents the NP couplings. Using the expression of the effective Hamiltonian Eq. (5) the decay amplitude for $B \to K_1 l^+ l^-$ is given by

$$\begin{aligned}
&\mathcal{M}(B\to K_1 l^+l^-) = \frac{\alpha G_F}{2\sqrt{2}\pi}V_{tb}V_{ts}^* \\
&\times\Big[\langle K_1(p_{K_1},\epsilon)|\bar{s}\gamma^\mu(1-\gamma_5)b|B(p_B)\rangle\Big\{(C_9^{eff}+R_V)\bar{l}\gamma_\mu l \\
&+(C_{10}+R_A)\bar{l}\gamma_\mu\gamma_5 l\Big\} + \langle K_1(p_{K_1},\epsilon)|\bar{s}\gamma^\mu(1+\gamma_5)b|B(p_B)\rangle \\
&\times\Big\{R'_V\bar{l}\gamma_\mu l + R'_A\bar{l}\gamma_\mu\gamma_5 l\Big\} \\
&-2\frac{C_7^{eff}}{s}m_b\langle K_1(p_{K_1},\epsilon)|\bar{s}i\sigma_{\mu\nu}q^\nu(1+\gamma_5)b|B(p_B)\rangle\bar{l}\gamma^\mu l \\
&+\langle K_1(p_{K_1},\epsilon)|\bar{s}(1+\gamma_5)b|B(p_B)\rangle\Big\{R_S\bar{l}l + R_P\bar{l}\gamma_5 l\Big\} \\
&+\langle K_1(p_{K_1},\epsilon)|\bar{s}\gamma^\mu(1-\gamma_5)b|B(p_B)\rangle\Big\{R'_S\bar{l}l + R'_P\bar{l}\gamma_5 l\Big\} \\
&+2C_T\langle K_1(p_{K_1},\epsilon)|\bar{s}\sigma_{\mu\nu}b|B(p_B)\rangle\bar{l}\sigma^{\mu\nu}l \\
&+2iC_{TE}\epsilon^{\mu\nu\alpha\beta}\langle K_1(p_{K_1},\epsilon)|\bar{s}\sigma_{\mu\nu}b|B(p_B)\rangle\bar{l}\sigma_{\alpha\beta}l\Big] \qquad (7)
\end{aligned}$$

Note: One can also consider the new physics contribution coming from the operator $O'_7 = C'_7\bar{s}\sigma^{\mu\nu}bLF^{\mu\nu}$. However, in the present study we do not include these effects.

A. Form Factors and Mixing of $K_1(1270) - K_1(1400)$

The hadronic matrix elements of quark operators appearing in Eq. (7) over the meson states, for the exclusive $B \to K_1(1270, 1400)\ell^+\ell^-$ decays can be parameterized in terms of the form factors as:

$$\langle K_1(p_{k_1},\varepsilon)\,|\bar{s}\gamma_\mu b|\,B(p_B)\rangle = -\Big[\varepsilon^*_\mu\,(m_B+m_{K_1})\,V_1(q^2) - (p_B+p_{k_1})_\mu\,(\varepsilon^*\cdot q)\,\frac{V_2(q^2)}{m_B+m_{K_1}}\Big] + q_\mu\,(\varepsilon\cdot q)\,\frac{2m_{K_1}}{q^2}\,\left[V_3(q^2)-V_0(q^2)\right] \tag{8}$$

$$\langle K_1(p_{k_1},\varepsilon)\,|\bar{s}\gamma_\mu\gamma_5 b|\,B(p_B)\rangle = \frac{2i\epsilon_{\mu\nu\alpha\beta}}{m_B+m_{K_1}}\varepsilon^{*\nu}p^\alpha_{k_1}q^\beta A(q^2) \tag{9}$$

where $p_B(p_{k_1})$ are the momenta of the $B(K_1)$ mesons and ε_μ correspond to the polarization of the final state axial vector K_1 meson. In Eq.(8) we have

$$V_3(q^2) = \frac{m_B+m_{K_1}}{2m_{K_1}}V_1(q^2) - \frac{m_B-m_{K_1}}{2m_{K_1}}V_2(q^2) \tag{10}$$

with

$$V_3(0) = V_0(0)$$

Additionally

$$\begin{aligned}\langle K_1\,|\bar{s}i\sigma_{\mu\nu}b|\,B\rangle &= [\varepsilon^*_\mu(p_B+p_{k_1})_\nu - \varepsilon^*_\nu(p_B+p_{k_1})_\mu]F_1(q^2)\\ &+ \left(\frac{m_B^2-m_{K_1}^2}{q^2}F_2(q^2)\right)(\varepsilon^*_\mu q_\nu - \varepsilon^*_\nu q_\mu)\\ &+ \left(\frac{F_2(q^2)}{q^2}+\frac{F_3(q^2)}{m_B^2-m_{K_1}^2}\right)\varepsilon^*\cdot q\\ &\times \left[(p_B+p_{k_1})_\nu q_\mu - (p_B+p_{k_1})_\mu q_\nu\right]\end{aligned} \tag{11}$$

$$\begin{aligned}&\langle K_1(p_{k_1},\varepsilon)\,|\bar{s}i\sigma_{\mu\nu}q^\nu b|\,B(p_B)\rangle\\ &= \left[\left(m_B^2-m_{K_1}^2\right)\varepsilon^*_\mu - (\varepsilon^*\cdot q)(p_B+p_{k_1})_\mu\right]F_2(q^2)\\ &+ (\varepsilon^*\cdot q)\left[q_\mu - \frac{q^2}{m_B^2-m_{K_1}^2}(p_B+p_{k_1})_\mu\right]F_3(q^2)\end{aligned} \tag{12a}$$

$$\langle K_1(p_{k_1},\varepsilon)\,|\bar{s}i\sigma_{\mu\nu}q^\nu\gamma_5 b|\,B(p_B)\rangle = -2i\epsilon_{\mu\nu\alpha\beta}\varepsilon^{*\nu}p^\alpha_{K_1}q^\beta F_1(q^2) \tag{12b}$$

with $F_1(0) = 2F_2(0)$. Where Eqs. (12a,12b) are obtained by contracting Eq. (11) with q^ν. Moreover, the matrix element $\langle K_1(p_{k_1},\varepsilon)|\bar{s}(1\pm\gamma_5)b|B(p_B)\rangle$ can be calculated by contracting Eq. (8) with q^μ and by making use of the equation of motions along with Eq. (10), we have

$$\langle K_1(p_{k_1},\varepsilon)|\bar{s}(1\pm\gamma_5)b|B(p_B)\rangle = \frac{1}{m_b}\left\{\pm 2m_{K_1}(\varepsilon^*\cdot q)V_0(q^2)\right\} \tag{13}$$

where the mass of strange quark has been neglected.

As the physical states $K_1(1270)$ and $K_1(1400)$ are mixed states of the K_{1A} and K_{1B} with mixing angle θ_K as defined in Eqs. (1-2). The $B\to K_1$ form factors can be parameterized as [22]

$$\begin{pmatrix}\langle K_1(1270)|\bar{s}\gamma_\mu(1-\gamma_5)b|B\rangle\\ \langle K_1(1400)|\bar{s}\gamma_\mu(1-\gamma_5)b|B\rangle\end{pmatrix} = M\begin{pmatrix}\langle K_{1A}|\bar{s}\gamma_\mu(1-\gamma_5)b|B\rangle\\ \langle K_{1B}|\bar{s}\gamma_\mu(1-\gamma_5)b|B\rangle\end{pmatrix}, \tag{14}$$

$$\begin{pmatrix}\langle K_1(1270)|\bar{s}\sigma_{\mu\nu}q^\mu(1+\gamma_5)b|B\rangle\\ \langle K_1(1400)|\bar{s}\sigma_{\mu\nu}q^\mu(1+\gamma_5)b|B\rangle\end{pmatrix} = M\begin{pmatrix}\langle K_{1A}|\bar{s}\sigma_{\mu\nu}q^\mu(1+\gamma_5)b|B\rangle\\ \langle K_{1B}|\bar{s}\sigma_{\mu\nu}q^\mu(1+\gamma_5)b|B\rangle\end{pmatrix}, \tag{15}$$

where the mixing matrix M is

$$M = \begin{pmatrix} \sin\theta_K & \cos\theta_K \\ \cos\theta_K & -\sin\theta_K \end{pmatrix}. \tag{16}$$

So the form factors A^{K_1}, $V^{K_1}_{0,1,2}$ and $F^{K_1}_{0,1,2}$ satisfy the following relations

$$\begin{pmatrix} \frac{A^{K_1(1270)}}{m_B+m_{K_1(1270)}} \\ \frac{A^{K_1(1400)}}{m_B+m_{K_1(1400)}} \end{pmatrix} = M \begin{pmatrix} \frac{A^{K_{1A}}}{m_B+m_{K_{1A}}} \\ \frac{A^{K_{1B}}}{m_B+m_{K_{1B}}} \end{pmatrix}, \tag{17}$$

$$\begin{pmatrix} (m_B+m_{K_1(1270)})V_1^{K_1(1270)} \\ (m_B+m_{K_1(1400)})V_1^{K_1(1400)} \end{pmatrix} = M \begin{pmatrix} (m_B+m_{K_{1A}})V_1^{K_{1A}} \\ (m_B+m_{K_{1B}})V_1^{K_{1B}} \end{pmatrix}, \tag{18}$$

$$\begin{pmatrix} \frac{V_2^{K_1(1270)}}{m_B+m_{K_1(1270)}} \\ \frac{V_2^{K_1(1400)}}{m_B+m_{K_1(1400)}} \end{pmatrix} = M \begin{pmatrix} \frac{V_2^{K_{1A}}}{m_B+m_{K_{1A}}} \\ \frac{V_2^{K_{1B}}}{m_B+m_{K_{1B}}} \end{pmatrix}, \tag{19}$$

$$\begin{pmatrix} m_{K_1(1270)}V_0^{K_1(1270)} \\ m_{K_1(1400)}V_0^{K_1(1400)} \end{pmatrix} = M \begin{pmatrix} m_{K_{1A}}V_0^{K_{1A}} \\ m_{K_{1B}}V_0^{K_{1B}} \end{pmatrix}, \tag{20}$$

$$\begin{pmatrix} F_1^{K_1(1270)} \\ F_1^{K_1(1400)} \end{pmatrix} = M \begin{pmatrix} F_1^{K_{1A}} \\ F_1^{K_{1B}} \end{pmatrix}, \tag{21}$$

$$\begin{pmatrix} (m_B^2-m^2_{K_1(1270)})F_2^{K_1(1270)} \\ (m_B^2+m^2_{K_1(1400)})F_2^{K_1(1400)} \end{pmatrix} = M \begin{pmatrix} (m_B^2-m^2_{K_{1A}})F_2^{K_{1A}} \\ (m_B^2-m^2_{K_{1B}})F_2^{K_{1B}} \end{pmatrix}, \tag{22}$$

$$\begin{pmatrix} \frac{F_3^{K_1(1270)}}{(m_B^2-m^2_{K_1(1270)})} \\ \frac{F_3^{K_1(1400)}}{(m_B^2-m^2_{K_1(1400)})} \end{pmatrix} = M \begin{pmatrix} \frac{F_3^{K_{1A}}}{(m_B^2-m^2_{K_{1A}})} \\ \frac{F_3^{K_{1B}}}{(m_B^2-m^2_{K_{1B}})} \end{pmatrix}, \tag{23}$$

where we have supposed that $p^\mu_{K_1(1270),K_1(1400)} \simeq p^\mu_{K_{1A},K_{1B}}$. Using the above matrix elements, the decay amplitude for $B \to K_1 l^+ l^-$ can be written as

$$\begin{aligned}
\mathcal{M}(B \to K_1 l^+ l^-) = \frac{\alpha G_F}{4\sqrt{2}\pi} V_{tb}V_{ts}^*(-i)\Bigg[& (\bar{l}\gamma_\mu l) \\
& \times\Big\{ -2\mathcal{A}\epsilon_{\mu\nu\alpha\beta}\epsilon^{*\nu}p^\alpha_{K_1}q^\beta - i\mathcal{B}_1\epsilon^*_\mu + i\mathcal{B}_2\varepsilon^*\cdot q(p_B+p_{K_1})_\mu\Big\} \\
& +(\bar{l}\gamma_\mu\gamma_5 l)\times\Big\{ -2\mathcal{C}_1\epsilon_{\mu\nu\alpha\beta}\epsilon^{*\nu}p^\alpha_{K_1}q^\beta - i\mathcal{D}_1\epsilon^*_\mu \\
& +i\mathcal{D}_2\varepsilon^*\cdot q(p_B+p_{K_1})_\mu + i\mathcal{D}_0\varepsilon^*\cdot q q_\mu\Big\} \\
& +i\mathcal{G}_1(\bar{l}l)\varepsilon^*\cdot q + i\mathcal{G}_2(\bar{l}\gamma_5 l)\varepsilon^*\cdot q \\
& +4i\mathcal{C}_{TE}\epsilon_{\mu\nu\alpha\beta}(\bar{l}\sigma^{\mu\nu}l)\Big\{\mathcal{G}_5\big(\varepsilon^{*\alpha}(p_B+p_{k_1})^\beta \\
& -\varepsilon^{*\beta}(p_B+p_{k_1})^\alpha\big) + \mathcal{G}_3(\varepsilon^{*\alpha}q^\beta - \varepsilon^{*\beta}q^\alpha) \\
& +\mathcal{G}_4\varepsilon^*\cdot q\big[(p_B+p_{k_1})^\beta q^\alpha - (p_B+p_{k_1})^\alpha q^\beta\big]\Big\} \\
& +4\mathcal{C}_T(\bar{l}\sigma_{\mu\nu}l)\Big\{\mathcal{G}_5\big(\varepsilon^{*\mu}(p_B+p_{k_1})^\nu \\
& -\varepsilon^{*\nu}(p_B+p_{k_1})^\mu\big) + \mathcal{G}_3(\varepsilon^{*\mu}q^\nu - \varepsilon^{*\nu}q^\mu) \\
& +\mathcal{G}_4\varepsilon^*\cdot q\big[(p_B+p_{k_1})^\nu q^\mu - (p_B+p_{k_1})^\mu q^\nu\big]\Big\}\Bigg]
\end{aligned} \tag{24}$$

The auxiliary functions appearing in (24) can be written as follows:

$$
\begin{aligned}
\mathcal{A} &= 2(C_9^{eff} + R_V + R'_V)\frac{A(q^2)}{m_B(1+\hat{k})} + \frac{4m_b C_7^{eff} F_1(q^2)}{q^2} \\
\mathcal{B}_1 &= 2(C_9^{eff} + R_V - R'_V)m_B(1+\hat{k})V_1(q^2) \\
&\quad +4m_b C_7^{eff}(1-\hat{k}^2)\frac{F_2(q^2)}{(q^2/m_B^2)} \\
\mathcal{B}_2 &= 2(C_9^{eff} + R_V - R'_V)\frac{V_2(q^2)}{m_B(1+\hat{k})} \\
&\quad +\frac{4m_b C_7^{eff}}{q^2}\left[F_2(q^2) + \frac{(q^2/m_B^2)}{(1-\hat{k}^2)}F_3(q^2)\right] \\
\mathcal{C}_1 &= 2(C_{10} + R_A + R'_A)\frac{A(q^2)}{m_B(1+\hat{k})} \\
\mathcal{D}_1 &= 2(C_{10} + R_A - R'_A)m_B(1+\hat{k})V_1(q^2) \\
\mathcal{D}_2 &= 2(C_{10} + R_A - R'_A)\frac{V_2(q^2)}{m_B(1+\hat{k})} \\
\mathcal{D}_0 &= \frac{4\hat{k}}{m_B}(C_{10} + R_A - R'_A)\frac{V_3(q^2) - V_0(q^2)}{(q^2/m_B^2)} \\
\mathcal{G}_1 &= -4(R_S - R'_S)\frac{\hat{k}}{(m_b/m_B)}V_0(q^2) \\
\mathcal{G}_2 &= -4(R_P - R'_P)\frac{\hat{k}}{(m_b/m_B)}V_0(q^2) \\
\mathcal{G}_3 &= \frac{m_B^2(1-\hat{k}^2)}{q^2}F_2(q^2) \\
\mathcal{G}_4 &= \frac{F_2(q^2)}{q^2} + \frac{F_3(q^2)}{m_B^2(1-\hat{k}^2)} \\
\mathcal{G}_5 &= F_1(q^2)
\end{aligned}
$$

where $q = (p_+ + p_-) = (p_B - p_{K_1})$ and $\hat{k} \equiv m_{K_1}/m_B$.

B. Phenomenological bounds on NP couplings

In the present paper, we use the constraints on the NP couplings parameters from A. Kumar *et al* [32]. However, for self consistency these bounds are given below:

In the absence of $R_{V,A}$ the bounds are

$$|R'_V|^2 + |R'_A|^2 \leq 16.8, \tag{25}$$

however these bounds are weakened when we include $R_{V,A}$

$$|R'_V|^2 + |R'_A|^2 \leq 39.7, \tag{26}$$

On the other hand the constraints on tensor coupling entirely come from $B(\bar{B} \to X_s\mu^+\mu^-)$ which are

$$|\mathcal{C}_T|^2 + 4|\mathcal{C}_{TE}|^2 \leq 1.3, \tag{27}$$

The limits on scalar and pseudo scalar couplings are extracted from $B(\bar{B}_s^0 \to \mu^+\mu^-)$

$$|R_S - R'_S|^2 + |R_P - R'_P|^2 \leq 0.44, \tag{28}$$

and from $B(\bar{B} \to X_s\mu^+\mu^-)$ [33, 34] are

$$|R_S|^2 + |R_P|^2 < 45, \qquad R'_s = R_S, \qquad R'_P = R_P. \tag{29}$$

III. ANALYTICAL CALCULATIONS OF DOUBLY POLARIZED FORWARD BACKWARD ASYMMETRIES

Now we have all the ingredients to calculate the physical observables. The double differential decay rate is given as[32]

$$\frac{d^2\Gamma(B\to K_1 l^+ l^-)}{d\cos\theta ds}=\frac{1}{2m_B}\frac{\rho\sqrt{\lambda}}{(8\pi)^3}|\mathcal{M}|^2 \tag{30}$$

where $\rho\equiv\sqrt{1-\frac{4m^2}{s}}$ and $\lambda\equiv m_B^4+m_{k_1}^4+s^2-2m_B^2m_{k_1}^2-2m_B^2s-2m_{k_1}^2s$. By using the expression of the decay amplitude given in Eq. (24) one can get the expression of the dilepton invariant mass spectrum as

$$\frac{d\Gamma(B\to K_1 l^+ l^-)}{ds}=\frac{G_F^2\alpha^2 m_B}{2^{14}\pi^5}|V_{tb}V_{ts}^*|^2\frac{\rho\sqrt{\lambda}}{(8\pi)^3}\delta \tag{31}$$

where

$$\begin{aligned}
\delta &= 4(2m^2+s)\{\frac{8\lambda}{3}|\mathcal{A}|^2+\frac{12m_{K_1}^2s+\lambda}{3m_{K_1}^2s}|\mathcal{B}_1|^2+\frac{\lambda t}{3m_{K_1}^2s}\mathcal{R}e(\mathcal{B}_1\mathcal{B}_2^*)+\frac{\lambda^2}{3m_{K_1}^2s}|\mathcal{B}_2|^2\}\\
&+\frac{32\lambda}{3}(s-4m^2)|\mathcal{C}_1|^2+[\frac{4\lambda(2m^2+s)}{3m_{K_1}^2s}+16(s-4m^2)]|\mathcal{D}_1|^2-8\frac{m^2\lambda}{m_{K_1}^2}\mathcal{R}e(\mathcal{D}_1\mathcal{D}_0^*)-\frac{4\lambda}{3m_{K_1}^2s}[(2m^2+s)\\
&\times(m_B^2-m_{K_1}^2)+s(s-4m^2)]\mathcal{R}e(\mathcal{D}_1\mathcal{D}_2^*)+[6m^2s(2m_B^2+2m_{K_1}^2-s)+\lambda(2m^2+s)]|\mathcal{D}_2|^2\\
&+\frac{8m^2\lambda}{m_{K_1}^2}(m_B^2-m_{K_1}^2)\mathcal{R}e(\mathcal{D}_2\mathcal{D}_0^*)+\frac{4m^2s\lambda}{m_{K_1}^2}|\mathcal{D}_0|^2-256m\lambda\mathcal{G}_5\mathcal{R}e(\mathcal{A}\mathcal{C}_{TE}^*)+\frac{32m}{m_{K_1}^2}\{\mathcal{G}_4\lambda t+\mathcal{G}_5(\lambda\\
&+12m_{K_1}^2(m_B^2-m_{K_1}^2))+\mathcal{G}_3(\lambda+12sm_{K_1}^2)\}\mathcal{R}e(\mathcal{B}_1\mathcal{C}_T^*)+\frac{32m\lambda}{m_{K_1}^2}(\mathcal{G}_5j+\mathcal{G}_3t+\mathcal{G}_4\lambda)\mathcal{R}e(\mathcal{B}_2\mathcal{C}_T^*)\\
&-\frac{4m\lambda}{m_{K_1}^2}\mathcal{R}e(\mathcal{D}_1\mathcal{G}_2^*)+\frac{4m\lambda(m_B^2-m_{K_1}^2)}{m_{K_1}^2}\mathcal{R}e(\mathcal{D}_2\mathcal{G}_2^*)+\frac{4ms\lambda}{m_{K_1}^2}\mathcal{R}e(\mathcal{D}_0\mathcal{G}_2^*)+\frac{(s-4m^2)\lambda}{m_{K_1}^2}|\mathcal{G}_1|^2\\
&+\frac{s\lambda}{m_{K_1}^2}|\mathcal{G}_2|^2-\frac{256}{3sm_{K_1}^2}\Big[\{12sm_{K_1}^2(8m^2((m_B^2+m_{K_1}^2)-4s)-2\lambda-2s(m_B^2+m_{K_1}^2)+s^2)\\
&+\lambda(4m^2-s)(s-8m_{K_1}^2)\}|\mathcal{G}_5|^2+(4m^2-s)s\{2\lambda j\mathcal{G}_4\mathcal{G}_5+\lambda^2|\mathcal{G}_4|^2+(24m_{K_1}^2(m_B^2-m_{K_1}^2)\\
&+13\lambda)\mathcal{G}_3\mathcal{G}_5+13t\lambda\mathcal{G}_3\mathcal{G}_4+12(\lambda+sm_{K_1}^2)|\mathcal{G}_3|^2\}\Big]|\mathcal{C}_{TE}|^2+\frac{64}{3sm_{K_1}^2}\Big[\{2\mathcal{G}_4\mathcal{G}_5sj+2\mathcal{G}_3\mathcal{G}_4st\\
&+s\lambda|\mathcal{G}_4|^2\}\lambda(8m^2+s)+\mathcal{G}_3\mathcal{G}_5s\{4m^2(2\lambda+24m_{K_1}^2(m_B^2-m_{K_1}^2))+4s(12m_{K_1}^2(m_B^2-m_{K_1}^2)+\lambda)\}\\
&+|\mathcal{G}_3|^2 4s(3m^2(2\lambda+8sm_{K_1}^2)+s(12sm_{K_1}^2+\lambda))+|\mathcal{G}_5|^2\{4m^2\Big(3s(\lambda-8m_{K_1}^2(s-2(m_B^2+m_{K_1}^2)))\\
&+(8m_{K_1}^2-s)\lambda\Big)+12sm_{K_1}^2(\lambda+(m_B^2-m_{K_1}^2)^2)+\lambda s(s-8m_{K_1}^2)\}\Big]|\mathcal{C}_T|^2
\end{aligned}$$

where $t\equiv -{m_B}^2+m_{K_1}^2+s$ and $j\equiv -m_B^2-3m_{K_1}^2+s$.

we first define the six orthogonal vectors belonging to the polarizations of l^- and l^+ which we denote here by S_i and W_i respectively where i =L, N and T corresponding to the longitudinally, Normally and transversally polarized lepton $l^\pm$ respectively. [18, 35, 36]

$$
\begin{aligned}
S_L^\mu &\equiv (0, \mathbf{e}_L) = \left(0, \frac{\mathbf{p}_-}{|\mathbf{p}_-|}\right) \\
S_N^\mu &\equiv (0, \mathbf{e}_N) = \left(0, \frac{\mathbf{p_{k_1}} \times \mathbf{p}_-}{|\mathbf{p_{k_1}} \times \mathbf{p}_-|}\right) \\
S_T^\mu &\equiv (0, \mathbf{e}_T) = (0, \mathbf{e}_N \times \mathbf{e}_L) \qquad (32) \\
W_L^\mu &\equiv (0, \mathbf{w}_L) = \left(0, \frac{\mathbf{p}_+}{|\mathbf{p}_+|}\right) \\
W_N^\mu &\equiv (0, \mathbf{w}_N) = \left(0, \frac{\mathbf{p_{k_1}} \times \mathbf{p}_+}{|\mathbf{p_{k_1}} \times \mathbf{p}_+|}\right) \\
W_T^\mu &\equiv (0, \mathbf{w}_T) = (0, \mathbf{w}_N \times \mathbf{w}_L) \qquad (33)
\end{aligned}
$$

where p_+, p_- and p_{K_1} denote the three momenta vectors of the final particles l^+, l^- and K_1 respectively. These polarization vectors $S_i^\mu(W_i^\mu)$ in Eqs. (32) and (33) are defined in the rest frame of $l^-(l^+)$. When we apply lorentz boost to bring these polarization vectors from rest frame of $l^-(l^+)$ to the centre of mass frame of l^+ and l^-, only the longitudinal polarization four vector get boosted while the other two polarization vectors remain unchanged. After this operation the longitudinal four vector read as

$$
\begin{aligned}
S_L^\mu &= \left(\frac{|p_-|}{m}, \frac{E_l \mathbf{p}_-}{m|\mathbf{p}_-|}\right) \\
W_L^\mu &= \left(\frac{|p_+|}{m}, -\frac{E_l \mathbf{p}_+}{m|\mathbf{p}_+|}\right) \qquad (34)
\end{aligned}
$$

To achieve the polarization asymmetries one can use the spin projector $\frac{1}{2}(1+\gamma_5 \not{S})$ for l^- and for the l^+ spin projector is $\frac{1}{2}(1+\gamma_5 \not{W})$. Normalized, unpolarized differential forward-backward asymmetry is defined as

$$
\mathcal{A}_{FB} = \frac{\int_0^1 \frac{d^2\Gamma}{ds d\cos\theta} d\cos\theta - \int_{-1}^0 \frac{d^2\Gamma}{ds d\cos\theta} d\cos\theta}{\int_0^1 \frac{d^2\Gamma}{ds d\cos\theta} d\cos\theta + \int_{-1}^0 \frac{d^2\Gamma}{ds d\cos\theta} d\cos\theta} \qquad (35)
$$

When the spins of both leptons are taken into account, the $\mathcal{A}_{FB}$ will be a function of the spins of final leptons, and is defined as

$$
\begin{aligned}
\mathcal{A}_{FB}^{ij} = \left(\frac{d\Gamma}{ds}\right)^{-1} \Big\{ \int_0^1 d\cos\theta - \int_{-1}^0 d\cos\theta \Big\} \\
\times \Big\{ \Big[\frac{d^2\Gamma(s^- = i, s^+ = j)}{ds d\cos\theta} - \frac{d^2\Gamma(s^- = i, s^+ = -j)}{ds d\cos\theta} \Big] \\
- \Big[\frac{d^2\Gamma(s^- = -i, s^+ = j)}{ds d\cos\theta} - \frac{d^2\Gamma(s^- = -i, s^+ = -j)}{ds d\cos\theta} \Big] \Big\} \qquad (36)
\end{aligned}
$$

$$
\begin{aligned}
\mathcal{A}_{FB}^{ij} = \mathcal{A}_{FB}(s^- = i, s^+ = j) - \mathcal{A}_{FB}(s^- = i, s^+ = -j) \\
- \mathcal{A}_{FB}(s^- = -i, s^+ = j) + \mathcal{A}_{FB}(s^- = -i, s^+ = -j) \qquad (37)
\end{aligned}
$$

Using these definitions for the double polarized FB asymmetries, we have found the expressions of numerators as follows:

$$
\begin{aligned}
\mathcal{A}_{FB}^{LL} &= \sqrt{s\lambda(s-4m^2)}\Big[4\big\{\mathcal{R}e(\mathcal{A}\mathcal{D}_1^*)+\mathcal{R}e(\mathcal{B}_1\mathcal{C}_1^*)\big\}\\
&+ \frac{2m}{m_{K_1}^2 s}\big\{t\mathcal{R}e(\mathcal{B}_1\mathcal{G}_1^*)+\lambda\mathcal{R}e(\mathcal{B}_2\mathcal{G}_1^*)\big\}+\frac{64}{s}\\
&\times \big((m_B^2-m_{K_1}^2)\mathcal{G}_5+s\mathcal{G}_3\big)\mathcal{R}e(\mathcal{C}_1\mathcal{C}_T^*)+\frac{32m}{m_{K_1}^2 s}\\
&\times \Big[(m_B^2-5m_{K_1}^2-s)\mathcal{G}_5-\mathcal{G}_3 t-\lambda\mathcal{G}_4\Big]\mathcal{R}e(\mathcal{D}_1\mathcal{C}_{TE}^*)\\
&+ \frac{8m}{m_{K_1}^2}\big(\mathcal{G}_5 j+\mathcal{G}_3 t+\lambda\mathcal{G}_4\big)\Big\{\frac{4(m_B^2-m_{K_1}^2)}{s}\\
&\times \mathcal{R}e(\mathcal{D}_2\mathcal{C}_{TE}^*)+4\mathcal{R}e(\mathcal{D}_0\mathcal{C}_{TE}^*)\\
&+ \frac{1}{m}\Big(\mathcal{R}e(\mathcal{G}_1\mathcal{C}_T^*)+2\mathcal{R}e(\mathcal{G}_2\mathcal{C}_{TE}^*)\Big)\Big\}\Big]
\end{aligned}
$$

$$
\begin{aligned}
\mathcal{A}_{FB}^{NN} &= \frac{m}{m_{K_1}^2}\sqrt{\frac{\lambda(s-4m^2)}{s}}\Big[-2\big(t\mathcal{R}e(\mathcal{B}_1\mathcal{G}_1^*)+\lambda\mathcal{R}e(\mathcal{B}_2\mathcal{G}_1^*)\big)\\
&- 32\big(\mathcal{G}_5 j+\mathcal{G}_3 t+\lambda\mathcal{G}_4\big)\big[\mathcal{R}e(\mathcal{D}_1\mathcal{C}_{TE}^*)\\
&- (m_B^2-m_{K_1}^2)\mathcal{R}e(\mathcal{D}_2\mathcal{C}_{TE}^*)-s\mathcal{R}e(\mathcal{D}_0\mathcal{C}_{TE}^*)\\
&+ \frac{s}{4m}\big\{\mathcal{R}e(\mathcal{G}_1\mathcal{C}_T^*)+2\mathcal{R}e(\mathcal{G}_2\mathcal{C}_{TE}^*)\big\}\big]\Big]
\end{aligned}
$$

$$
\begin{aligned}
\mathcal{A}_{FB}^{TT} &= \frac{2m}{m_{K_1}^2}\sqrt{\frac{\lambda(s-4m^2)}{s}}\Big[t\mathcal{R}e(\mathcal{B}_1\mathcal{G}_1^*)+\lambda\mathcal{R}e(\mathcal{B}_2\mathcal{G}_1^*)\\
&+ 16\big(\mathcal{G}_5 j+\mathcal{G}_3 t+\lambda\mathcal{G}_4\big)\Big\{\mathcal{R}e(\mathcal{D}_1\mathcal{C}_{TE}^*)\\
&- (m_B^2-m_{K_1}^2)\mathcal{R}e(\mathcal{D}_2\mathcal{C}_{TE}^*)-s\mathcal{R}e(\mathcal{D}_0\mathcal{C}_{TE}^*)\\
&+ \frac{s}{4m}\big(\mathcal{R}e(\mathcal{G}_1\mathcal{C}_T^*)-2\mathcal{R}e(\mathcal{G}_2\mathcal{C}_{TE}^*)\big)\Big\}\Big]
\end{aligned}
$$

$$
\begin{aligned}
\mathcal{A}_{FB}^{LT} &= \frac{8\lambda}{3\sqrt{s}}\Big[8(s+4m^2)\mathcal{G}_5\mathcal{R}e(\mathcal{A}\mathcal{C}_{TE}^*)-ms|\mathcal{A}|^2\\
&- 1024m|\mathcal{G}_5|^2|\mathcal{C}_{TE}|^2-4(s-4m^2)\mathcal{G}_5\mathcal{R}e(\mathcal{C}_1\mathcal{C}_T^*)\\
&+ \frac{1}{m_{K_1}^2}\Big\{m\Big(|\mathcal{B}_1|^2+t\mathcal{R}e(\mathcal{B}_1\mathcal{B}_2^*)+\lambda|\mathcal{B}_2|^2\Big)\\
&+ (\mathcal{G}_3+\mathcal{G}_5+\mathcal{G}_4 t)\big\{2(s+4m^2)\mathcal{R}e(\mathcal{B}_1\mathcal{C}_T^*)\\
&- 4(s-4m^2)\mathcal{R}e(\mathcal{D}_1\mathcal{C}_{TE}^*)\big\}\\
&+ (\mathcal{G}_5 j+\mathcal{G}_3 t+\mathcal{G}_4\lambda)\big\{2(s+4m^2)\mathcal{R}e(\mathcal{B}_2\mathcal{C}_T^*)\\
&- 4(s-4m^2)\mathcal{R}e(\mathcal{D}_2\mathcal{C}_{TE}^*)\big\}\\
&+ 64m\big[|\mathcal{G}_5|^2(s-4m_{K_1}^2)+2s(\mathcal{G}_5\mathcal{G}_3+\mathcal{G}_5\mathcal{G}_4 j\\
&+ \mathcal{G}_3\mathcal{G}_4 t)+s|\mathcal{G}_3|^2+s\lambda|\mathcal{G}_4|^2\big]|\mathcal{C}_T|^2\Big\}\Big]
\end{aligned}
$$

$$
\begin{aligned}
\mathcal{A}_{FB}^{TL} &= \frac{8\lambda}{3\sqrt{s}}\Big[ms|\mathcal{A}|^2 - 8(s+4m^2)\mathcal{G}_5\mathcal{R}e(\mathcal{A}\mathcal{C}_{TE}^*) \\
&+ 1024m|\mathcal{G}_5|^2|\mathcal{C}_{TE}|^2 - 4(s-4m^2)\mathcal{G}_5\mathcal{R}e(\mathcal{C}_1\mathcal{C}_T^*) \\
&+ \frac{1}{m_{K_1}^2}\Big\{-m\Big(|\mathcal{B}_1|^2 + t\mathcal{R}e(\mathcal{B}_1\mathcal{B}_2^*) + \lambda|\mathcal{B}_2|^2\Big) \\
&- (\mathcal{G}_3+\mathcal{G}_5+\mathcal{G}_4 t)\big\{2(s+4m^2)\mathcal{R}e(\mathcal{B}_1\mathcal{C}_T^*) \\
&+ 4(s-4m^2)\mathcal{R}e(\mathcal{D}_1\mathcal{C}_{TE}^*)\big\} \\
&- (\mathcal{G}_5 j + \mathcal{G}_3 t + \mathcal{G}_4\lambda)\big\{2(s+4m^2)\mathcal{R}e(\mathcal{B}_2\mathcal{C}_T^*) \\
&+ 4(s-4m^2)\mathcal{R}e(\mathcal{D}_2\mathcal{C}_{TE}^*)\big\} \\
&- 64m\big[|\mathcal{G}_5|^2(s-4m_{K_1}^2) + 2s(\mathcal{G}_5\mathcal{G}_3 + \mathcal{G}_5\mathcal{G}_4 j \\
&+ \mathcal{G}_3\mathcal{G}_4 t) + s|\mathcal{G}_3|^2 + s\lambda|\mathcal{G}_4|^2\big]|\mathcal{C}_T|^2\Big\}\Big]
\end{aligned}
$$

$$
\begin{aligned}
\mathcal{A}_{FB}^{NT} &= \frac{m^2\sqrt{\lambda}}{m_{K_1}^2 s}\Big[4t\big\{(m_B^2 - m_{K_1}^2)\mathcal{I}m(\mathcal{B}_1\mathcal{D}_2^*) - \mathcal{I}m(\mathcal{B}_1\mathcal{D}_1^*) \\
&+ s\mathcal{I}m(\mathcal{B}_1\mathcal{D}_0^*) + \frac{s}{2m}\mathcal{I}m(\mathcal{B}_1\mathcal{G}_2^*)\big\} \\
&+ 4\lambda\big\{(m_B^2 - m_{K_1}^2)\mathcal{I}m(\mathcal{B}_2\mathcal{D}_2^*) - \mathcal{I}m(\mathcal{B}_2\mathcal{D}_1^*) \\
&+ s\mathcal{I}m(\mathcal{B}_2\mathcal{D}_0^*) + \frac{s}{2m}\mathcal{I}m(\mathcal{B}_2\mathcal{G}_2^*)\big\}\Big]
\end{aligned}
$$

$$
\mathcal{A}_{FB}^{NT} = -\mathcal{A}_{FB}^{TN} \tag{38}
$$

$$
\begin{aligned}
\mathcal{A}_{FB}^{LN} &= \frac{4\lambda\sqrt{s-4m^2}}{3}\Big[8\mathcal{G}_5\mathcal{I}m(\mathcal{A}\mathcal{C}_T^*) - m\mathcal{I}m(\mathcal{A}\mathcal{C}_1^*) \\
&+ \frac{1}{m_{K_1}^2 s}\Big\{m\big(\mathcal{I}m(\mathcal{B}_1\mathcal{D}_1^*) + t(\mathcal{I}m(\mathcal{B}_1\mathcal{D}_2^*) + \mathcal{I}m(\mathcal{B}_2\mathcal{D}_1^*)) \\
&+ \lambda\mathcal{I}m(\mathcal{B}_2\mathcal{D}_2^*)\big) + 4s(\mathcal{G}_3+\mathcal{G}_5)\big(2\mathcal{I}m(\mathcal{B}_1\mathcal{C}_{TE}^*) + 2t\mathcal{I}m(\mathcal{B}_2\mathcal{C}_{TE}^*)\big)\Big\}\Big]
\end{aligned}
$$

$$
\begin{aligned}
\mathcal{A}_{FB}^{NL} &= \frac{4\lambda\sqrt{s-4m^2}}{3}\Big[-8\mathcal{G}_5\mathcal{I}m(\mathcal{A}\mathcal{C}_T^*) - m\mathcal{I}m(\mathcal{A}\mathcal{C}_1^*) \\
&+ \frac{1}{m_{K_1}^2 s}\Big\{m\big(\mathcal{I}m(\mathcal{B}_1\mathcal{D}_1^*) + t(\mathcal{I}m(\mathcal{B}_1\mathcal{D}_2^*) + \mathcal{I}m(\mathcal{B}_2\mathcal{D}_1^*)) + \lambda\mathcal{I}m(\mathcal{B}_2\mathcal{D}_2^*)\big)\Big\} \\
&- \frac{8}{m_{K_1}^2}\Big\{(\mathcal{G}_3+\mathcal{G}_5+t\mathcal{G}_4)\mathcal{I}m(\mathcal{B}_1\mathcal{C}_{TE}^*) + (\mathcal{G}_5 j + \mathcal{G}_3 t + \mathcal{G}_4\lambda)\mathcal{I}m(\mathcal{B}_2\mathcal{C}_{TE}^*)\Big\}\Big]
\end{aligned}
$$

Note: It is worthful to mention here we have included short distance part, $Y_{SD}(z,\hat{s})$, of C_9^{effSM} in our numerical calculation which contains also the imaginary part, therefore, in $\mathcal{A}_{FB}^{NT}(\mathcal{A}_{FB}^{TN})$ and $\mathcal{A}_{FB}^{LN}(\mathcal{A}_{FB}^{NL})$ only those terms contribute which contain auxiliary functions A, B_1 and B_2.

IV. NUMERICAL RESULTS AND DISCUSSION

In this section we examine the effects of different new physics operators on polarized lepton pair forward-backward asymmetries. For this purpose, we analyze the behaviour of polarized *FB* asymmetries and their average values in the presence of constraints on NP couplings that are given in section II B. Regarding this, different scenarios for NP Lorentz structure are displayed in Table IV-VI. Numerical values of different input parameters are given in Table I, while the SM Wilson coefficients at $\mu = m_b$ are given in Table II. In addition to calculate the numerical values of observables under consideration, we have used the light-cone QCD sum rules form factors [38], summarized in Table III. The momentum dependence dipole parametrization for these form factors is:

$$
\mathcal{T}_i^X(q^2) = \frac{\mathcal{T}_i^X(0)}{1 - a_i^X\,(q^2/m_B^2) + b_i^X\,(q^2/m_B^2)^2}. \tag{39}
$$

TABLE I: Default values of input parameters used in the calculations [33]

$m_B = 5.28$ GeV, $m_b = 4.28$ GeV, $m_\mu = 0.105$ GeV,
$m_\tau = 1.77$ GeV, $f_B = 0.25$ GeV, $\lvert V_{tb}V_{ts}^*\rvert = 45 \times 10^{-3}$,
$\alpha^{-1} = 137$, $G_F = 1.17 \times 10^{-5}$ GeV^{-2},
$\tau_B = 1.54 \times 10^{-12}$ sec, $m_{K_1(1270)} = 1.270$ GeV,
$m_{K_1(1400)} = 1.403$ GeV, $m_{K_{1A}} = 1.31$ GeV,
$m_{K_{1B}} = 1.34$ GeV.

where $\mathcal{T}$ denotes the A, V or F form factors and the subscript i can take the value 0, 1, 2 or 3. The superscript X belongs to K_{1A} or K_{1B} state.

TABLE II: The Wilson coefficients C_i^μ at the scale $\mu \sim m_b$ in the SM [37].

C_1	C_2	C_3	C_4	C_5	C_6	C_7	C_9	C_{10}
1.107	-0.248	-0.011	-0.026	-0.007	-0.031	-0.313	4.344	-4.669

Before proceeding to analyze the NP, first we would like to mention here that the authors of ref [30, 39] concluded that all observables such as branching ratio, forward backward and single lepton polarization asymmetries, etc for $B \to K_1(1430)\mu^+\mu^-$ are sensitive to mixing angle θ_K. In this context, it is interesting to see the dependence of the values of double lepton polarizations forward-backward asymmetries on mixing angle θ_K. In this study, we have found that $\mathcal{A}_{FB}^{LL}$, $\mathcal{A}_{FB}^{LT}$ and $\mathcal{A}_{FB}^{TL}$ are sensitive to θ_K for the decay $B \to K_1(1430)\mu^+\mu^-$ as shown in fig 11(a-c) but not much sensitive for $B \to K_1(1270)\mu^+\mu^-$. Therefore, besides te other observables, the precise measurements of these asymmetries (for former decay channel) at LHC may also provide help to put some stringent constraint on the mixing angle θ_K in near future. However, as it is mentioned in ref. [40] that the branching ratio for $K_1(1430)$ is two order suppressed i.e. $Br(B \to K_1(1270)\mu^+\mu^-(\tau^+\tau^-))$ are of the order of $10^{-6}(10^{-8})$ while $Br(B \to K_1(1430)\mu^+\mu^-(\tau^+\tau^-))$ are of the order of $10^{-8}(10^{-10})$. For this reason we are not interested in the results of $B \to K_1(1430)\mu^+\mu^-(\tau^+\tau^-)$.

Now to see the behaviour of double polarized FB asymmetries under the influence of new physics couplings, we have drawn the s-dependence of these asymmetries in figs. 1-10. In all these graphs the grey shaded band corresponds to the region of the SM values of these asymmetries due to uncertainties in mixing angle θ_K while dashed line corresponds to the SM value when the central values of the form factors are taken. In fig. 1 (6) we present the dependence of $\mathcal{A}_{FB}^{LL}$ on s for the decay $B \to K_1(1270)\mu^+\mu^-$ ($B \to K_1(1270)\tau^+\tau^-$) when only vector type couplings are switched on. figs. 1a-1c depict the effects of different NP scenarios presented in tables (IV,V) on s dependence of $\mathcal{A}_{FB}^{LL}$. These figures show that the zero position of $\mathcal{A}_{FB}^{LL}$ shifts towards left and right-side of the corresponding SM value within allowed values of different NP coefficients. For example fig. 1a depicts scenario S1(see Table IV), where by fixing the value of R_A, three different curves of $\mathcal{A}_{FB}^{LL}$ are drawn within the allowed range of R_V. It shows that zero position of $\mathcal{A}_{FB}^{LL}$ shifts towards left and right-side of the corresponding SM value for all allowed values of R_V in S1 scenario. Similarly figs. 1b and 1c depict scenarios S4 and S6 given in table V. figs. 2a-2c depict the effects of tensor interactions (table VI) on s dependence of $\mathcal{A}_{FB}^{LL}$. For instance fig. 2c shows the case of S9 when both tensor couplings C_T and C_{TE} are present with opposite polarity. It is important to mention here that only those scenarios of all NP couplings are shown in figures for which the zero position of $\mathcal{A}_{FB}^{LL}$ is shifted distinctly in comparison to that of the zero position in SM. In contrast to $B \to K_1(1270)\mu^+\mu^-$, $\mathcal{A}_{FB}^{LL}$ does not have zero crossing for $B \to K_1(1270)\tau^+\tau^-$. figs. 6(a-c) depict scenarios S1, S4, S6 and fig. 7(a-c) depict scenarios S7, S8 and S9 which show, respectively, the possible effects

TABLE III: $B \to K_{1A,1B}$ form factors [38], where a and b are the parameters of the form factors in dipole parametrization.

$\mathcal{T}_i^X(q^2)$	$\mathcal{T}(0)$	a	b	$\mathcal{T}_i^X(q^2)$	$\mathcal{T}(0)$	a	b
$V_1^{K_{1A}}$	0.34	0.635	0.211	$V_1^{K_{1B}}$	-0.29	0.729	0.074
$V_2^{K_{1A}}$	0.41	1.51	1.18	$V_2^{K_{1B}}$	-0.17	0.919	0.855
$V_0^{K_{1A}}$	0.22	2.40	1.78	$V_0^{K_{1B}}$	-0.45	1.34	0.690
$A^{K_{1A}}$	0.45	1.60	0.974	$A^{K_{1B}}$	-0.37	1.72	0.912
$F_1^{K_{1A}}$	0.31	2.01	1.50	$F_1^{K_{1B}}$	-0.25	1.59	0.790
$F_2^{K_{1A}}$	0.31	0.629	0.387	$F_2^{K_{1B}}$	-0.25	0.378	-0.755
$F_3^{K_{1A}}$	0.28	1.36	0.720	$F_3^{K_{1B}}$	-0.11	1.61	10.2

TABLE IV: Scenarios for different possible fixed values of R_A, when only R_A and R_V couplings are present

Scenario	R_A	R_V
S1	-1.10	$-6.5 \leq R_V \leq 1$
S2	9	$-6.5 \leq R_V \leq 1$

TABLE V: Scenarios for different possible fixed values of R'_V and R'_A, when only R'_V and R'_A couplings are present

Scenario	R'_A	R'_V
S3	$-3 \leq R'_A \leq 3$	0.1
S4	$-3 \leq R'_A \leq 3$	2.75
S5	0.1	$-3 \leq R'_V \leq 3$
S6	2.75	$-3 \leq R'_V \leq 3$

when only vector and tensor type couplings are present in $\mathcal{A}_{FB}^{LL}$ for $B \to K_1(1270)\tau^+\tau^-$. In all these scenarios the value of $\mathcal{A}_{FB}^{LL}$ remains positive in high s region as predicted by SM value except S7. fig. 7a shows that when tensor coupling C_T is present only (Scenario S7), $\mathcal{A}_{FB}^{LL}$ can get the negative values in opposite to SM prediction. Therefore, if negative values of $\mathcal{A}_{FB}^{LL}$ are measured in future experiments for $B \to K_1(1270)\tau^+\tau^-$, these results will be unambiguous indication of existence of new physics beyond the SM (i.e. existence of tensor type interactions).

In figs. 3(a-d) and 4(a-c), we present the dependence of $\mathcal{A}_{FB}^{LT}$ on s for muons as final state leptons while figs. 8(a-c) and 9(a-c) show the dependence of $\mathcal{A}_{FB}^{LT}$ on s for tauons as final state leptons. fig 3a (8a) presents S1 (i.e when only R_A and R_V couplings are present), where three different curves for $\mathcal{A}_{FB}^{LT}$ are plotted by fixing $R_A = -1.10$ and by taking three different values of R_V within the allowed range (i.e. $-6.5 \leq R_V \leq 1$) for the case of muons (tauons) as final state doubly polarized leptons. This figure tells us that zero position of $\mathcal{A}_{FB}^{LT}$ gets shifted towards left and right with respect to SM zero position for all the different selected values of R_V with the allowed range while fig. 8a shows the NP effects when tauons are the final state leptons. One can also see from this figure that NP effects are significant. Similarly figs. 3b-3d present the NP effects on $\mathcal{A}_{FB}^{LT}$ when scenarios S2, S5 and S6 are considered for the decay $B \to K_1(1270)\mu^+\mu^-$. One can also notice from the expressions given in $\mathcal{A}_{FB}^{LT}(\mathcal{A}_{FB}^{TL})$ that $\mathcal{A}_{FB}^{LT} = -\mathcal{A}_{FB}^{TL}$ when we consider only vector type couplings. Therefore the effects of vector type couplings on $\mathcal{A}_{FB}^{TL}$ are same as $\mathcal{A}_{FB}^{LT}$. Moreover, figs. 4a-4c (9a-9c) present scenarios S7, S8 and S9 for the case of muons (tauons) as final state leptons when tensor type couplings, C_T and C_{TE}, are considered. For instance, fig. 4c represents scenario S9 (i.e. when both tensor interactions are present) in which we consider the case when both C_T and C_{TE} are present with opposite polarity. All these figures show that $\mathcal{A}_{FB}^{LT}$ is greatly effected by NP couplings in particular to tensor interactions. Furthermore, for the case of tauons, when different new physics couplings are switched on, for some of the cases $\mathcal{A}_{FB}^{LT}$ gets opposite value in entire high s region as compared to its SM values predictions.

Similar to $\mathcal{A}_{FB}^{LT}$, s dependence of $\mathcal{A}_{FB}^{TL}$ for different scenarios is shown in figs. 5(a-c) for the decay $B \to K_1(1270)\mu^+\mu^-$ while figs. 10(a-c) present for the case of tauons as final state leptons. figs. 5(a-c) show the effects of tensor type interactions (S7, S8 and S9). These figures show that all these new physics scenarios effect the s dependence value of $\mathcal{A}_{FB}^{TL}$ significantly. Additionally, figs. 10(a-c) manifest scenarios S7, S8 and S9 for the case of tauons. Again from these figures we conclude that different NP couplings modify the value of $\mathcal{A}_{FB}^{TL}$ significantly in the high s region.

It is emphasized here that in our analysis only $\mathcal{A}_{FB}^{LL}$, $\mathcal{A}_{FB}^{LT}$ and $\mathcal{A}_{FB}^{TL}$ are observed to be considerably effected by NP couplings of different types. Therefore the other remaining polarized lepton pair forward-backward asymmetries are not discussed.

Moreover, we eliminate the dependence of forward-backward polarized asymmetries on s by performing integration over s and find the average values of above mentioned asymmetries which are also experimentally useful tools to explore the new physics. We calculate the averaged double lepton polarization forward-backward asymmetries by

TABLE VI: Different Scenarios when tensor couplings are present

Scenario	C_T	C_{TE}
S7	$-1.14 \leq C_T \leq 1.14$	0
S8	0	$-0.57 \leq C_{TE} \leq 0.57$
S9	± 0.54	$-0.5 \leq C_{TE} \leq 0.5$

using the following formula

$$\langle \mathcal{A}_{FB}^{ij} \rangle = \frac{\int_{4m^2}^{(m_B - m_{K_1})^2} \mathcal{A}_{FB}^{ij} \frac{d\Gamma}{ds} ds}{\int_{4m^2}^{(m_B - m_{K_1})^2} \frac{d\Gamma}{ds} ds} \tag{40}$$

As mentioned in Sec. II that in the calculation of average values we do not include long distance contribution, $Y_{LD}(z, \hat{s})$. Now we discuss the effects of NP on $\langle \mathcal{A}_{FB}^{ij} \rangle$, in the following sections.

A. Tensor type interactions present only

In this section, we discuss the explicit dependence of tensor type couplings on the average values of different polarized forward-backward asymmetries. For this purpose 12e and 12f show the effects of NP tensor and axial tensor operators, respectively, on $\langle \mathcal{A}_{FB}^{ij} \rangle$ for the case of muons. fig.12e depicts the scenario S7 (see Table-VI. i.e. when C_T present only), in which $\langle \mathcal{A}_{FB}^{LL} \rangle$ significantly varies from its SM value. The value of $\langle \mathcal{A}_{FB}^{LL} \rangle$ increases and reaches to a maximum value of ≈ 0.21 and then again decreases within the allowed range ($-1.14 \leq C_T \leq 1.14$). It is also clear that $\langle \mathcal{A}_{FB}^{LL} \rangle$ does not change its sign while $\langle \mathcal{A}_{FB}^{LT} \rangle$ and $\langle \mathcal{A}_{FB}^{TL} \rangle$ both change their sign in the allowed range. Moreover, $\langle \mathcal{A}_{FB}^{LT} \rangle$ and $\langle \mathcal{A}_{FB}^{TL} \rangle$ show opposite trend such that $\langle \mathcal{A}_{FB}^{LT} \rangle$ ($\langle \mathcal{A}_{FB}^{TL} \rangle$) remains positive (negative) for ($-1.14 \leq C_T \leq -0.05$) while it becomes negative (positive) for ($-0.05 \leq C_T \leq 1.14$). All other polarized forward-backward asymmetries are insignificant for scenario S7. When only second type of tensor interaction C_{TE} is switched on (Scenario S8), fig. 12f manifest its possible effects on $\langle \mathcal{A}_{FB}^{ij} \rangle$. It can be easily noted here that only $\langle \mathcal{A}_{FB}^{LL} \rangle$ does not change its sign while all other change their sign, when C_{TE} is varied from -0.57 to 0.57. One can also observe that only $\langle \mathcal{A}_{FB}^{LL} \rangle$, $\langle \mathcal{A}_{FB}^{TL} \rangle$ and $\langle \mathcal{A}_{FB}^{LT} \rangle$ are effected significantly similar to the case when only C_T type interaction is swithced on. Similar to figs. 12e and 12f, we plot avaraged double lepton polarization forward-backward asymmetries in figs. 13e and 13f for the case of tauons, when only tensor type interactions are present. fig. 13e shows S7 scenario, where $\langle \mathcal{A}_{FB}^{ij} \rangle$ is plotted for the allowed range of C_T. From this plot we see that $\langle \mathcal{A}_{FB}^{LL} \rangle$, $\langle \mathcal{A}_{FB}^{LT} \rangle$ and $\langle \mathcal{A}_{FB}^{TL} \rangle$, are greatly influenced by NP tensor operator C_T as compared to their SM values, where by signs of some of these polarized forward-backward asymmetries are flipped as well. In comparison to this fig. 13f shows even more distinct effects on the values of all $\langle \mathcal{A}_{FB}^{ij} \rangle$ except $\langle \mathcal{A}_{FB}^{TN} \rangle$, $\langle \mathcal{A}_{FB}^{NT} \rangle$, $\langle \mathcal{A}_{FB}^{LN} \rangle$ and $\langle \mathcal{A}_{FB}^{NL} \rangle$ (not included), observed for S8, when only C_{TE} operator is switched on.

B. R_V and R_A couplings present only

When only R_V and R_A couplings are present, for the case of muons, figs. 12a and 12b represent scenarios S1 and S2 respectively. In fig. 12a, When the value of $R_A = -1.10$ is fixed and R_V is varied in allowed range from -6.5 to 1, $\langle \mathcal{A}_{FB}^{LL} \rangle$ is drastically changed from its SM value, while $\langle \mathcal{A}_{FB}^{LT} \rangle$ and $\langle \mathcal{A}_{FB}^{TL} \rangle$ are also modified appreciably from their SM values. The value of $\langle \mathcal{A}_{FB}^{LL} \rangle$ remains negative for the values of R_V from -6 to -3 and it acquires positive values for ($-3 \leq R_V \leq 1$), where the maximum value $\langle \mathcal{A}_{FB}^{LL} \rangle = 0.24$ is observed at $R_V = 1$. It is also clear from this plot that $\langle \mathcal{A}_{FB}^{LT} \rangle$ and $\langle \mathcal{A}_{FB}^{TL} \rangle$ follow the opposite pattern, such that $\langle \mathcal{A}_{FB}^{LT} \rangle$ ($\langle \mathcal{A}_{FB}^{TL} \rangle$) remains positive (negative) for ($-6 \leq R_V \leq -1.2$) and negative (positive) from -1.2 to 1. Similarly when S2 is considered (fig. 12b), all three double polarization FB asymmetries, $\langle \mathcal{A}_{FB}^{LL} \rangle$, $\langle \mathcal{A}_{FB}^{LT} \rangle$ and $\langle \mathcal{A}_{FB}^{TL} \rangle$ not only vary in magnitude for the allowed region of R_V but also change their polarities, where $\langle \mathcal{A}_{FB}^{LL} \rangle$ becomes positive to negative at $R_V = -3$ whereas $\langle \mathcal{A}_{FB}^{LT} \rangle$ ($\langle \mathcal{A}_{FB}^{TL} \rangle$) changes its sign from positive (negative) to negative (positive) at $R_V \approx -1.2$. All other averaged polarized FB asymmetries which are left out show negligible NP effects. When the case of tauons is considered, figs. 13a and 13b, it is observed that presence of couplings R_V and R_A effect $\langle \mathcal{A}_{FB}^{LL} \rangle$, $\langle \mathcal{A}_{FB}^{LT} \rangle$ and $\langle \mathcal{A}_{FB}^{TL} \rangle$, significantly. One can observe from fig. 13a that the magnitude of $\langle \mathcal{A}_{FB}^{LL} \rangle$, varies significantly within the allowed range ($-6 \leq R_V \leq 1$) along with the change in polarity of $\langle \mathcal{A}_{FB}^{LL} \rangle$. While when we consider S2 (fig. 13b), it shows the opposite behaviour for $\langle \mathcal{A}_{FB}^{LL} \rangle$, while similar behaviour for $\langle \mathcal{A}_{FB}^{LT} \rangle$ and $\langle \mathcal{A}_{FB}^{TL} \rangle$ as compared to S1.

C. R'_V and R'_A couplings present only

When only R'_V and R'_A couplings are present, figs. 12c and 12d depict scenarios s4 and s6 respectively for muons, while figs. 13c and 13d represent the case of tauons. Again from these figures, one can observe that only $\langle \mathcal{A}_{FB}^{LL} \rangle$, $\langle \mathcal{A}_{FB}^{LT} \rangle$ and $\langle \mathcal{A}_{FB}^{TL} \rangle$ are considerably effected for the case of muons as well as for the case of tauons in the presence of R'_V and R'_A couplings. In fig. 12c $\langle \mathcal{A}_{FB}^{LL} \rangle$ and $\langle \mathcal{A}_{FB}^{LT} \rangle$ acquire only positive sign where by $\langle \mathcal{A}_{FB}^{TL} \rangle$ acquire only negative

sign for all allowed values of R'_A. For S6 (fig. 12d), $\langle \mathcal{A}_{FB}^{LL} \rangle$ increases from 0.03 at $R'_V = -3$ and reaches to a maximum value of ≈ 0.23 at $R'_V = 3$ whereas $\langle \mathcal{A}_{FB}^{LT} \rangle$ and $\langle \mathcal{A}_{FB}^{TL} \rangle$ follow the opposite fashion, compared to s4. For the case of tauons, fig. 13c show that when we switch on only R'_V and R'_A, only $\langle \mathcal{A}_{FB}^{LL} \rangle > \langle \mathcal{A}_{FB}^{LL} \rangle_{SM}$ and $\langle \mathcal{A}_{FB}^{LT} \rangle > \langle \mathcal{A}_{FB}^{LT} \rangle_{SM}$ is true for all allowed values of R'_A, and $\langle \mathcal{A}_{FB}^{TL} \rangle < \langle \mathcal{A}_{FB}^{TL} \rangle_{SM}$ for entire allowed range $(-3 \leq R'_A \leq 3)$. Similar conclusion can be drawn from fig. 13d (S6) such as $\langle \mathcal{A}_{FB}^{LL} \rangle > \langle \mathcal{A}_{FB}^{LL} \rangle_{SM}$ for $(0.7 \leq R'_V \leq 3)$ while $\langle \mathcal{A}_{FB}^{LL} \rangle < \langle \mathcal{A}_{FB}^{LL} \rangle_{SM}$ for $(-3 \leq R'_V \leq 0.7)$. Also polarities of $\langle \mathcal{A}_{FB}^{LT} \rangle$ and $\langle \mathcal{A}_{FB}^{TL} \rangle$ are flipped.

V. CONCLUSION

In conclusion, we calculate double polarized *FB* asymmetries using most general model independent form of the effective Hamiltonian including all possible non-standard local four-fermi interactions. Our analysis shows that similar to the other observables, polarized *FB* asymmetries are also sensitive to the mixing angle θ_K. While considering the different NP scenarios our analysis exhibit that the averaged double lepton polarization forward-backward asymmetries are very sensitive to NP couplings. The key points are as under.

When vector axial-vector couplings are considered for the decay $B \to K_1(1270)\mu^+\mu^-$, only averaged polarized forward-backward asymmetries, $\langle \mathcal{A}_{FB}^{LL} \rangle$, $\langle \mathcal{A}_{FB}^{LT} \rangle$ and $\langle \mathcal{A}_{FB}^{TL} \rangle$ are effected significantly whereas all other averaged polarized *FB* asymmetries are suppressed. Similarly when only tensor interaction C_T is present again $\langle \mathcal{A}_{FB}^{LL} \rangle$, $\langle \mathcal{A}_{FB}^{LT} \rangle$ and $\langle \mathcal{A}_{FB}^{TL} \rangle$ are modified considerably as compared to their SM values while $\langle \mathcal{A}_{FB}^{LL} \rangle$, $\langle \mathcal{A}_{FB}^{NN} \rangle$, $\langle \mathcal{A}_{FB}^{TT} \rangle$, $\langle \mathcal{A}_{FB}^{LT} \rangle$ and $\langle \mathcal{A}_{FB}^{TL} \rangle$ are influenced greatly when only C_{TE} coupling is present. In similarity to the decay $B \to K_1(1270)\mu^+\mu^-$, when the case of tauons is considered it is found again that $\langle \mathcal{A}_{FB}^{LL} \rangle$, $\langle \mathcal{A}_{FB}^{LT} \rangle$ and $\langle \mathcal{A}_{FB}^{TL} \rangle$ are modified as compared to their SM values, when either vector axial-vector operators or tensor interactions of type C_T are present only. Moreover all types of averaged doubly polarized *FB* asymmetries except $\langle \mathcal{A}_{FB}^{LN}, \rangle$, $\langle \mathcal{A}_{FB}^{NL} \rangle$, $\langle \mathcal{A}_{FB}^{NT} \rangle$ and $\langle \mathcal{A}_{FB}^{TN} \rangle$ are influenced greatly when only C_{TE} tensor couplings are switched on.

Additionally, the dependence of polarized lepton pair forward-backward asymmetries $\mathcal{A}_{FB}^{LL}$, $\mathcal{A}_{FB}^{LT}$ and $\mathcal{A}_{FB}^{TL}$ on s for the decay $B \to K_1(1270)\mu^+\mu^-$ depict the left and right-side shifting of zero crossing positions of these forward-backward polarized asymmetries from their corresponding SM values, when vector axial-vector and tensor type NP operators are considered. Moreover, signs of some of these polarized *FB* asymmetries are also flipped for few allowed values of different NP couplings. Similar conclusion is drawn for the case of tauons as final state leptons.

Acknowledgments

The authors would like to thank Prof. Fayyazuddin for their valuable guidance and useful discussions. One of the author I. Ahmed. would like to acknowledge the grant (2013/23177-3) from FAPESP.

[1] T. Goto, Y. Okada, Y. Shimizu and M. Tanaha, Phys. Rev. D **55**, 4273 (1997) [arXiv:hep-ph/9609512].
[2] S. Bertolini, F. Borzumati, A. Masiero and G. Ridolfi, Nucl. Phys. B **353**, 591 (1991).
[3] C. S. Lim, T. Morozumi and A. I. Sanda, Phys. Lett. B **218**, 343 (1989); X.-G. He, T. D. Nguyen and R. R. Volkas, Phys. Rev. D **38**, 814 (1988); B. Grinstein, M. J. Savage and M. B. Wise, Nucl. Phys. B **319** 271 (1989); Y. G. Kim, P. Ko and J. S. Lee, Nucl. Phys. B **544**, 64 (1999) [arXiv:hep-ph/9810336]; C.-S. Huang, W.-J. Huo and Y.-L. Wu, Mod. Phys. Lett. A **14**, 2453 (1999) [arXiv:hep-ph/9911203].
[4] N. G. Deshpande, J. Trampetic and K. Panose, Phys. Rev. D **39**, 1461 (1989) ; P. J. O'Donnell and H. K. K. Tung, Phys. Rev. D **43**, R2067 (1991); N. Paver and Riazuddin, Phys. Rev. D **45**, 978 (1992); W.-S. Hou, R.S. Willey and A. Soni, Phys. Rev. Lett. **58**, 1608 (1987) [Erratum-ibid. **60**, 2337 (1987)].
[5] A. Ali, T. Mannel and T. Morozumi, Phys. Lett. B **273**, 505 (1991).
[6] A. Ali, E. Lunghi, C. Greub and G. Hiller, Phys. Rev. D **66**, 034002 (2002) [arXiv:hep-ph/0112300].
[7] T. M. Aliev, M. K. Cakmak and M. Savci, Nucl. Phys. B **607**, 305 (2001) [arXiv:hep-ph/0009133]; T. M. Aliev, A. Ozpineci, M. Savci and C. Yuce, Phys. Rev. D **66**, 115006 (2002) [arXiv:hep-ph/0208128]; T. M. Aliev, A. Ozpineci and M. Savci, Phys. Lett. B **511**, 49 (2001) [arXiv:hep-ph/0103261]; T. M. Aliev and M. Savci, Phys. Lett. B **481**, 275 (2000) [arXiv:hep-ph/0003188]; T. M. Aliev, D. A. Demir and M. Savci, Phys. Rev. D **62**, 074016 (2000) [arXiv:hep-ph/9912525]; T. M. Aliev, C. S. Kim and Y. G. Kim, Phys. Rev. D **62**, 014026 (2000) [arXiv:hep-ph/9910501]; T. M. Aliev, E.O. Iltan, Phys. Lett. B **451**, 175 (1999) [arXiv:hep-ph/9804458].
[8] C.-H. Chen, C. Q. Geng, Phys. Rev. D **66**, 034006 (2002) [arXiv:hep-ph/0207038]; C.-H. Chen, C. Q. Geng, Phys. Rev. D **66**, 014007 (2002) [arXiv:hep-ph/0205306].
[9] G. Erkol, G. Turan, Nucl. Phys. B **635**, 286 (2002) [arXiv:hep-ph/0204219]; E. O. Iltan, G. Turan and I. Turan, J. Phys. G **28**, 307 (2002) [arXiv:hep-ph/0106136].

[10] W.-J. Li, Y.-B. Dai and C.-S. Huang, Eur. Phys. J. C **40**, 565 (2005) [arXiv:hep-ph/0410317].
[11] Q.-S. Yan, C.-S. Huang, W. Liao and S.-H. Zhu, Phys. Rev. D **62**, 094023 (2000) [arXiv:hep-ph/0004262].
[12] F. Kruger, E. Lunghi, Phys. Rev. D **63**, 014013 (2001) [arXiv:hep-ph/0008210].
[13] R. Mohanta, A. K. Giri, Phys. Rev. D **75**, 035008 (2007) [arXiv:hep-ph/0611068].
[14] S. R. Choudhury, N. Gaur and N. Mahajan, Phys. Rev. D **66**, 054003 (2002) [arXiv:hep-ph/0203041]; S. R. Choudhury, N. Gaur, [arXiv:hep-ph/0205076]; S. R. Choudhury, N. Gaur, [arXiv:hep-ph/0207353].
[15] T. M. Aliev, V. Bashiry and M. Savci, Phys. Rev. D **71**, 035013 (2005) [arXiv:hep-ph/0411327].
[16] U. O. Yilmaz, B. B. Sirvanli and G. Turan, Nucl. Phys. B **692**, 249 (2004) [arXiv:hep-ph/0407006]; U. O. Yilmaz, B. B. Sirvanli and G. Turan, Eur. Phys. J. C **30**, 197 (2003) [arXiv:hep-ph/0304100].
[17] S. R. Choudhury, N. Gaur, Phys. Lett. B **451**, 86 (1999) [arXiv:hep-ph/9810307]; J. K. Mizukoshi, X. Tata and Y. Wang, Phys. Rev. D **66**, 115003 (2002) [arXiv:hep-ph/0208078]; A. J. Buras, P. H. Chankowski, J. Rosiek and L. Slawianowska, Nucl. Phys. B **659**, 3 (2003) [arXiv:hep-ph/0210145]; A. J. Buras, P. H. Chankowski, J. Rosiek and L. Slawianowska, Phys. Lett. B **546**, 96 (2002) [arXiv:hep-ph/0207241].
[18] W. Bensalem, D. London, N. Sinha and R. Sinha, Phys. Rev. D **67**, 034007 (2003) [arXiv:hep-ph/0209228].
[19] S. R. Choudhury, N. Gaur, A. S. Cornell and G.C. Joshi, Phys. Rev. D **68**, 054016 (2003) [hep-ph/0304084].
[20] T. M. Aliev, V. Bashiry and M. Savci, Eur. Phys. J. C **35**, 197 (2004) [arXiv:hep-ph/0311294].
[21] T. M. Aliev, V. Bashiry, and M. Savci, Phys. Rev. D **72**, 034031 (2005) [arXiv:hep-ph/0506239].
[22] V. Bashiry, JHEP **0906**, 062 (2009) [arXiv:0902.2578 [hep-ph]].
[23] S. Ishaq, F. Munir and I. Ahmed, JHEP **07**, 006 (2013) .
[24] T. M. Aliev, V. Bashiry, M. Savci, JHEP **05**, 037 (2004) [arXiv:hep-ph/0403282].
[25] V. Bashiry, F. Falahati, Phys. Rev. D **77**, 015001 (2008) [arXiv:0707.3242v1 [hep-ph]].
[26] S. R. Choudhury, A. S. Cornell, N. Gaur and G. C. Joshi, Phys. Rev. D **69**, 054018 (2004) [arXiv:hep-ph/0307276].
[27] T. M. Aliev, V. Bashiry and M. Savci, Phys. Rev. D **73**, 034013 (2006) [arXiv:hep-ph/0504213].
[28] T. M. Aliev, V. Bashiry and M. Savci, Eur. Phys. J. C **40**, 505 (2005) [arXiv:hep-ph/0412384].
[29] M. Suzuki, Phys. Rev. D **47**, 1252 (1993); L. Burakovsky, J. T. Goldman, Phys. Rev. D **57**, 2879 (1998) [arXiv:9703271 [hep-ph]]; H. Y. Cheng, Phys. Rev. D **67**, 094007 (2003) [arXiv: 0301198 [hep-ph]].
[30] H. Hatanaka, K. C. Yang, Phys. Rev. D **77**, 094023 (2003) [arXiv:0804.3198 [hep-ph]]; H. Hatanaka, K. C. Yang, Phys. Rev. D **78**, 074007 (2008) [arXiv:0808.3731 [hep-ph]].
[31] A. J. Buras and M. Munz, Phys, Rev. D **52**, 186 (1995) [arXiv:hep-ph/9501281]; N. G. Deshpande and J. Trampetic, Phys. Rev. Lett. **60**, 2583 (1988); M. Misiak, Nucl. Phys. B **393**, 23 (1993) [Erratum-ibid. **439**, 461 (1995)].
[32] A. K. Alok, A. Dighe, D. Ghosh, D. London, J. Matias, M. Nagashima and A. Szynkman, JHEP **1002**, 053 (2010) [arXiv:0912.1382 [hep-ph]].
[33] K.A. Olive *et al.* (Particle Data Group), Chin. Phys. C **38**, 090001 (2014).
[34] C. Aubin, [arXiv:0909.2686 [hep-lat]].
[35] F. Kruger and L. M. Sehgal, Phys. Lett. B **380**, 199 (1996) [arXiv:hep-ph/9603237].
[36] S. Fukae, C. S. Kim and T. Yoshikawa, Phys. Rev. D **61**, 074015 (2000) [arXiv:hep-ph/9908229].
[37] A. Ali, P. Ball, L. T. Handoko and G. Hiller, Phys. Rev. D **61**, 074024 (2000) [arXiv:hep-ph/9910221].
[38] K. C. Yang, Phys. Rev. D **78**, 034018 (2008) [arXiv:0807.1171].
[39] Y. Li, J. Hua, K.-C. Yang, Eur. Phys. J. C **71**, 1775 (2011) [arXiv:hep-ph/1107.0630v2].
[40] A. Ahmed, I. Ahmed, M. Ali Paracha and A. Rehman, Phys. Rev. D **84**, 033010 (2011) [arXiv:1105.3887 [hep-ph]].

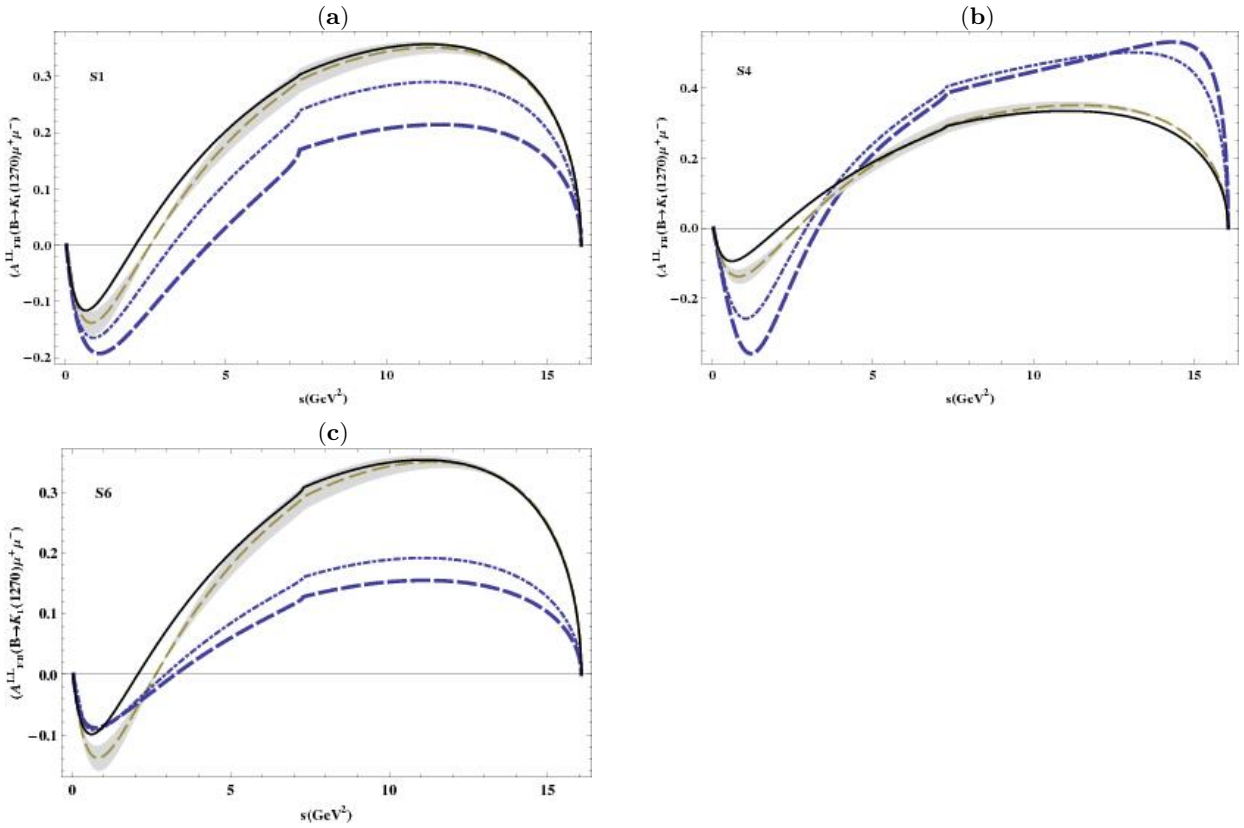

FIG. 1: The dependence of A_{FB}^{LL} on s for the decay $B \to K_1(1270)\mu^+\mu^-$, where the dashed-dotted, solid and dashed curves in each figure correspond to A_{FB}^{LL} for three different allowed values of vector type couplings.

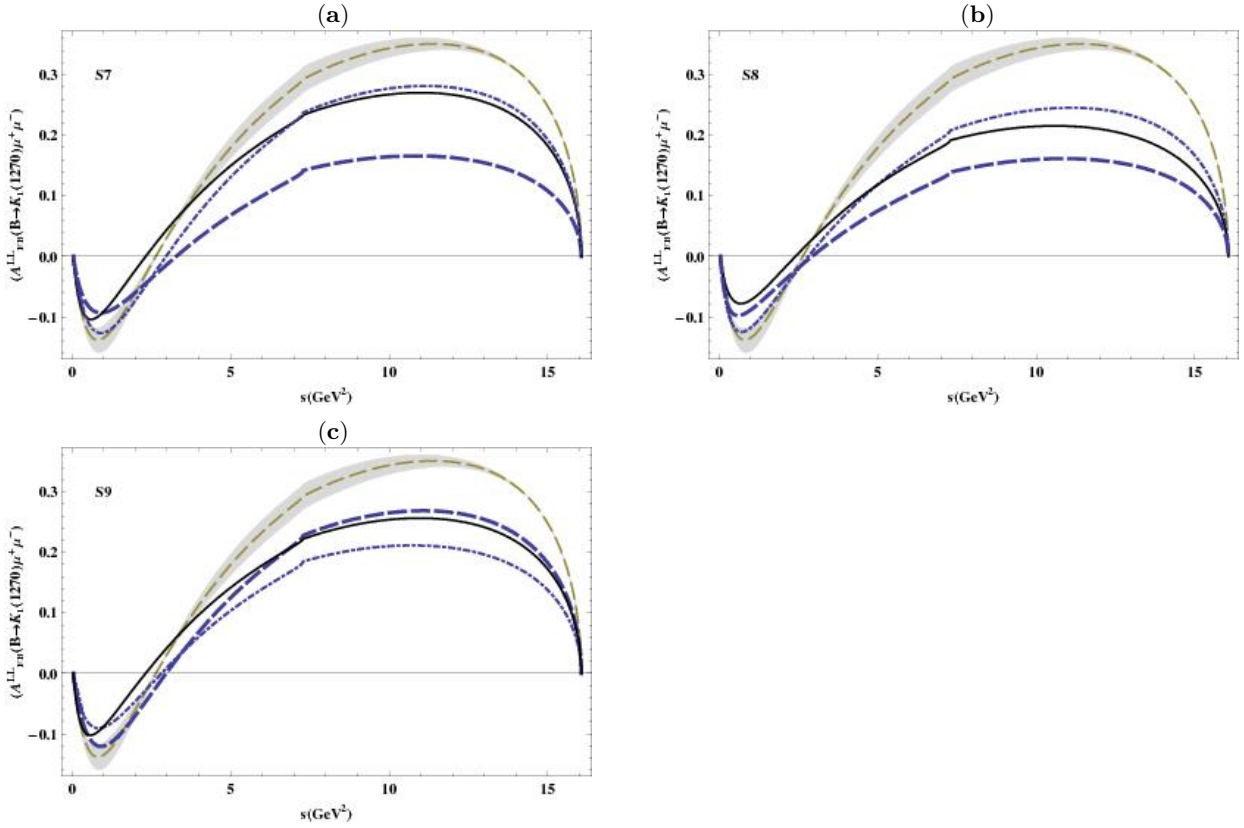

FIG. 2: The same as in figure 1, but for tensor type couplings.

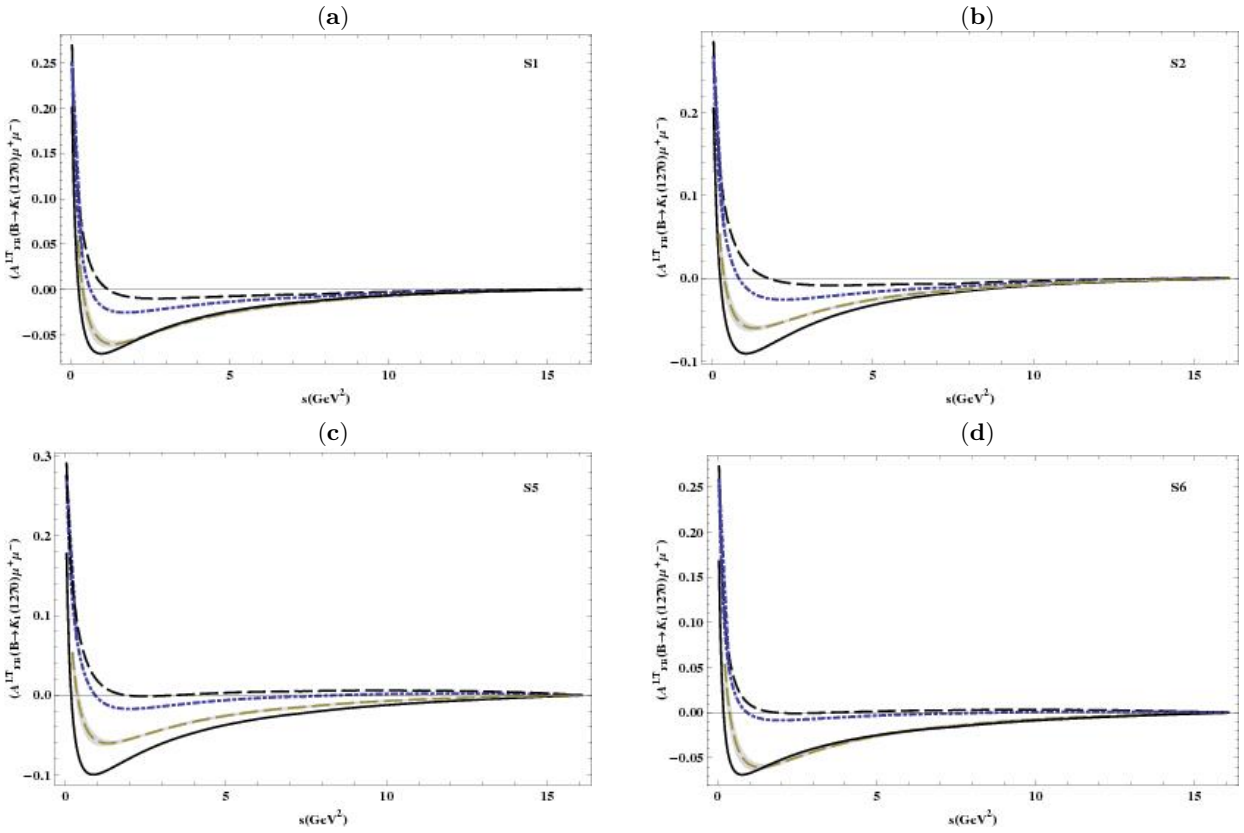

FIG. 3: The same as in figure 1, but for A_{FB}^{LT}.

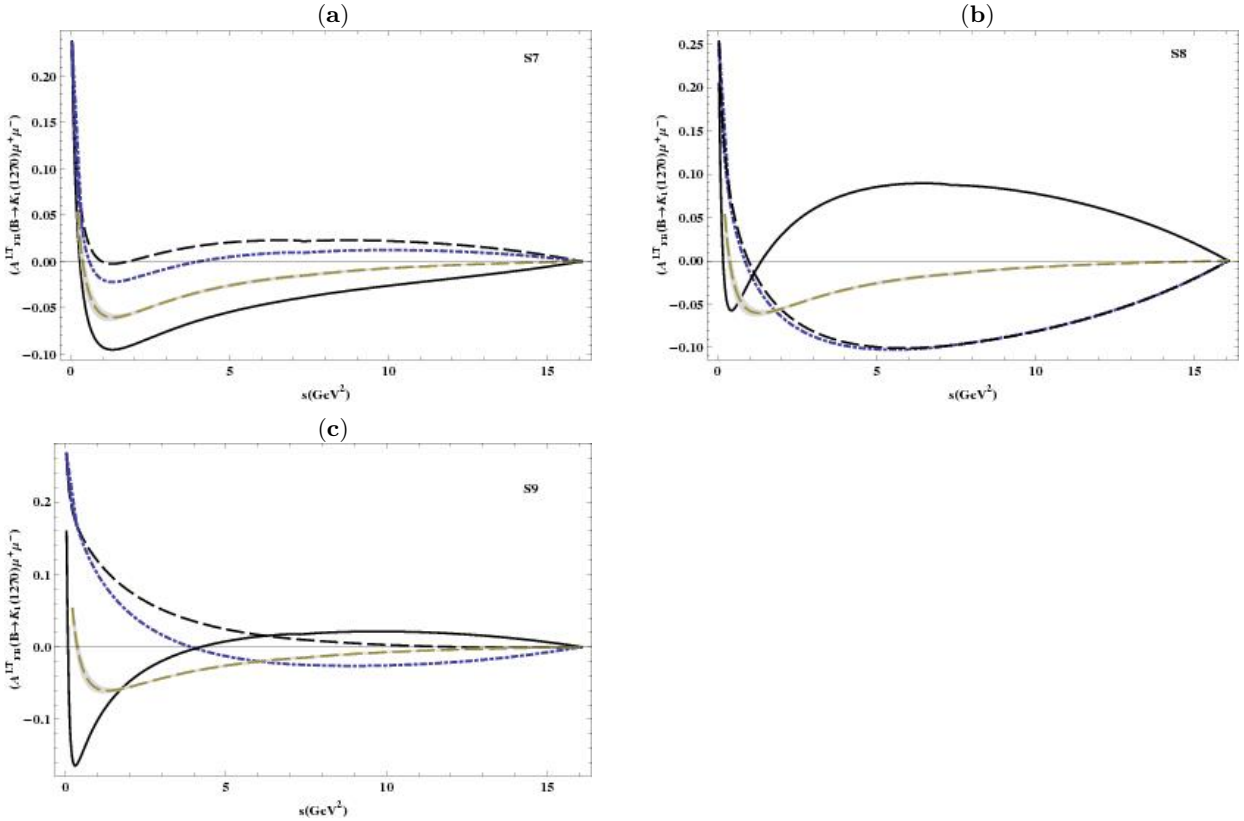

FIG. 4: The same as in figure 3, but for tensor type interactions.

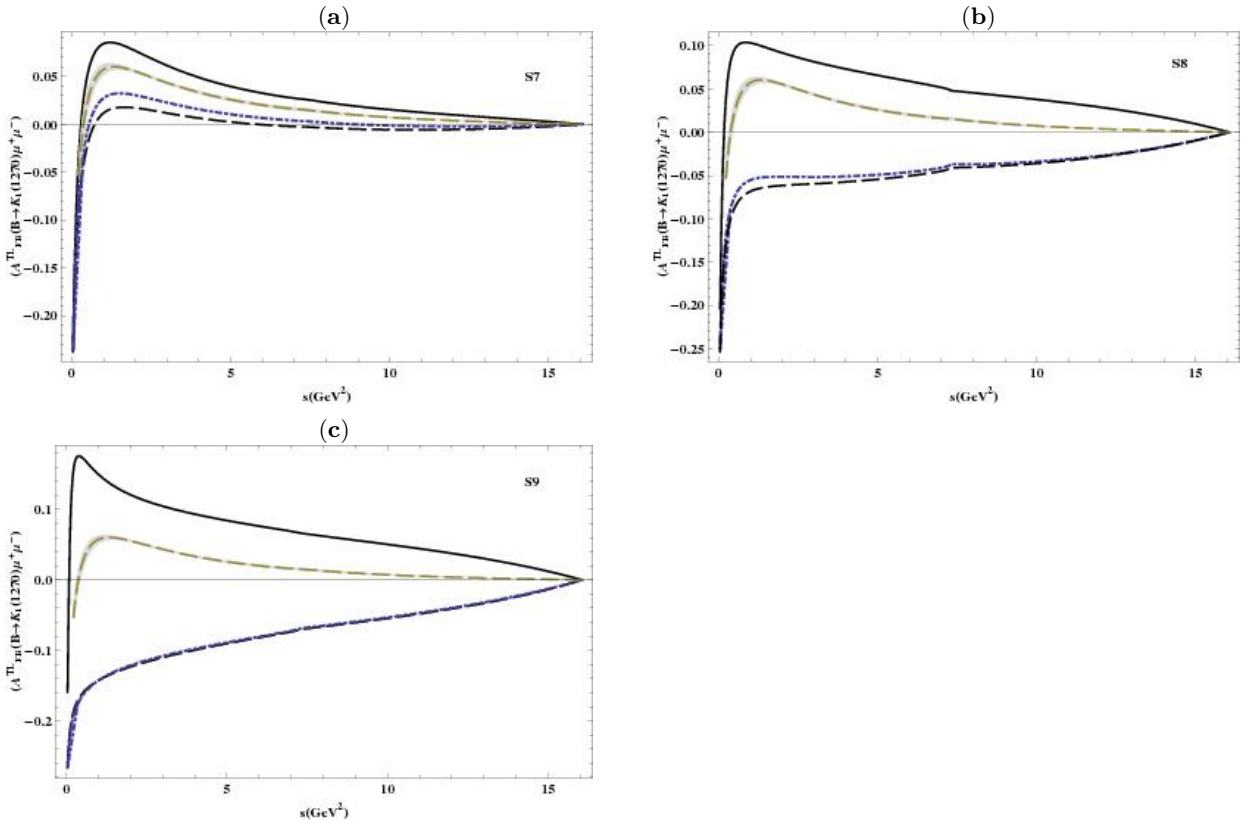

FIG. 5: The dependence of A_{FB}^{TL} on s for the decay $B \to K_1(1270)\mu^+\mu^-$, where the dashed-dotted, solid and dashed curves in each figure correspond to A_{FB}^{TL} for three different allowed values of tensor type couplings.

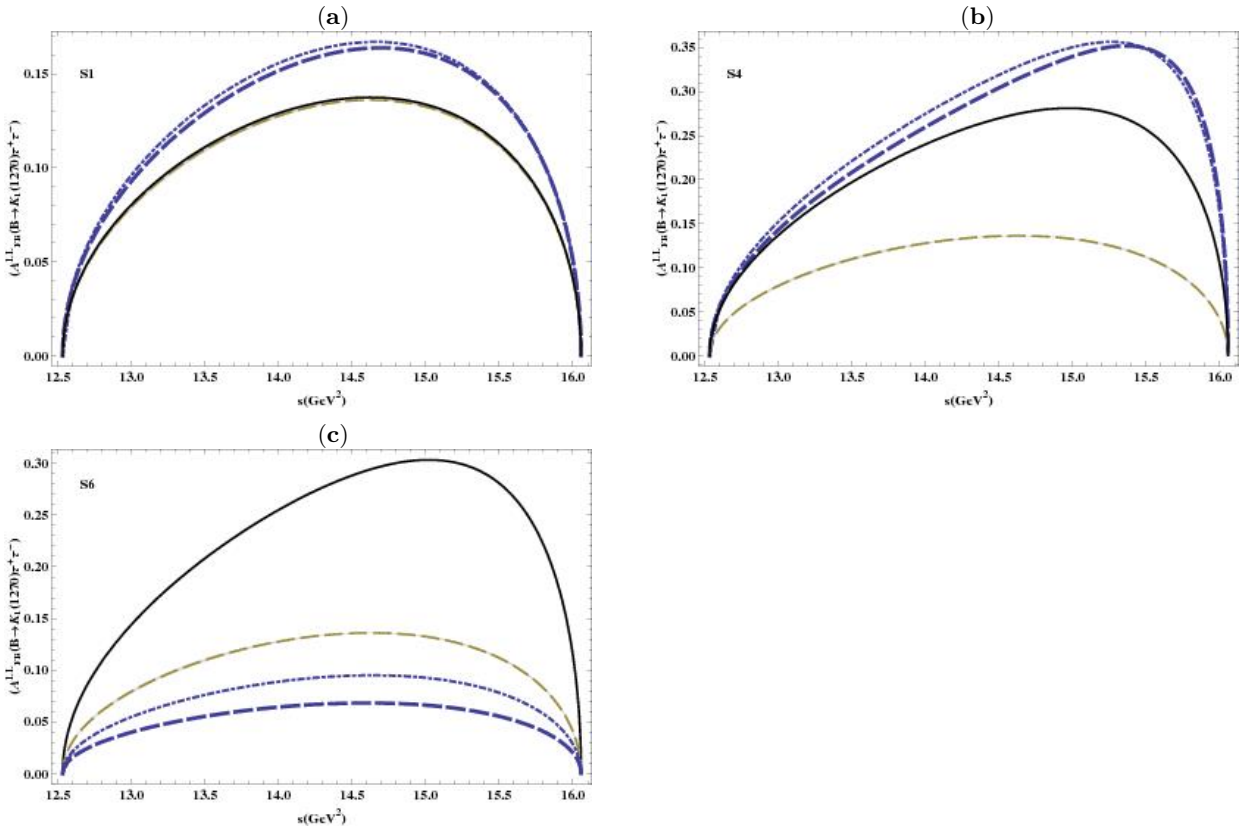

FIG. 6: The same as in figure 1, but for $B \to K_1(1270)\tau^+\tau^-$.

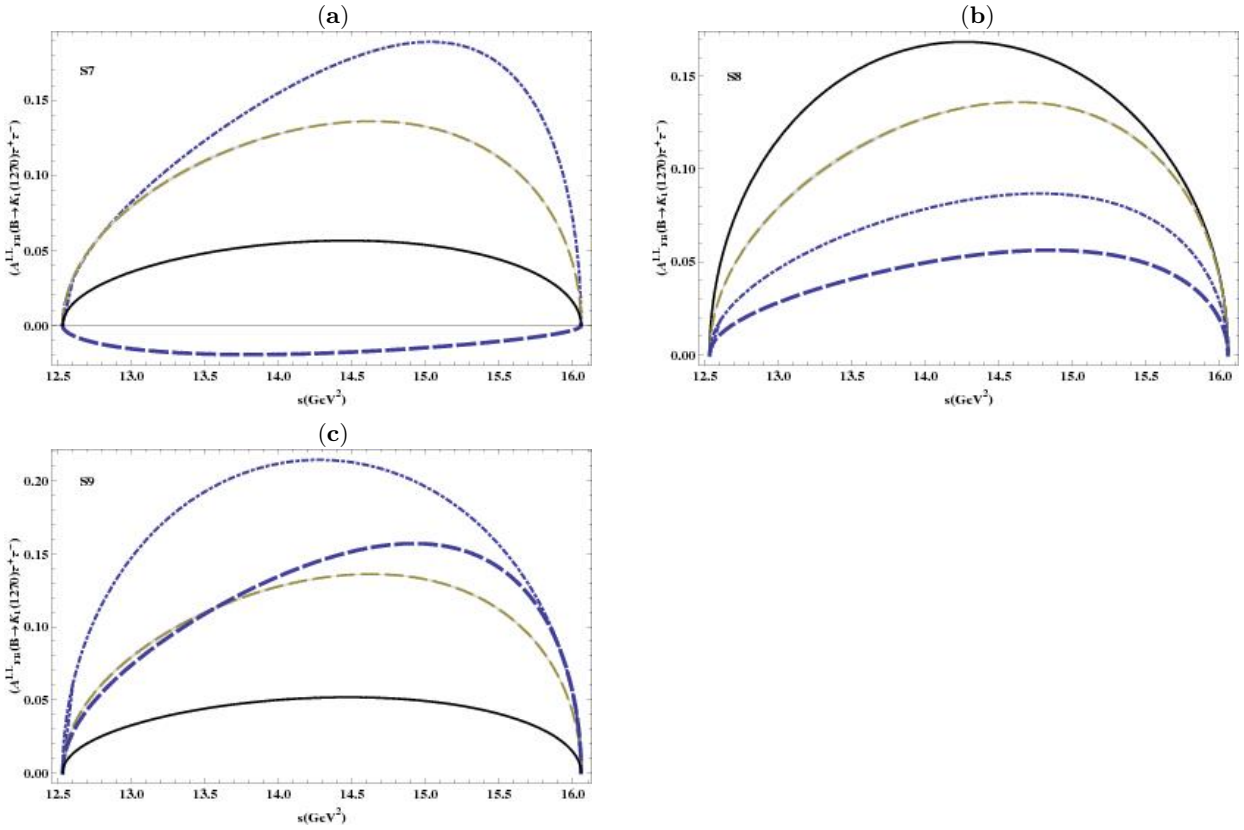

FIG. 7: The same as in figure 2, but for $B \to K_1(1270)\tau^+\tau^-$.

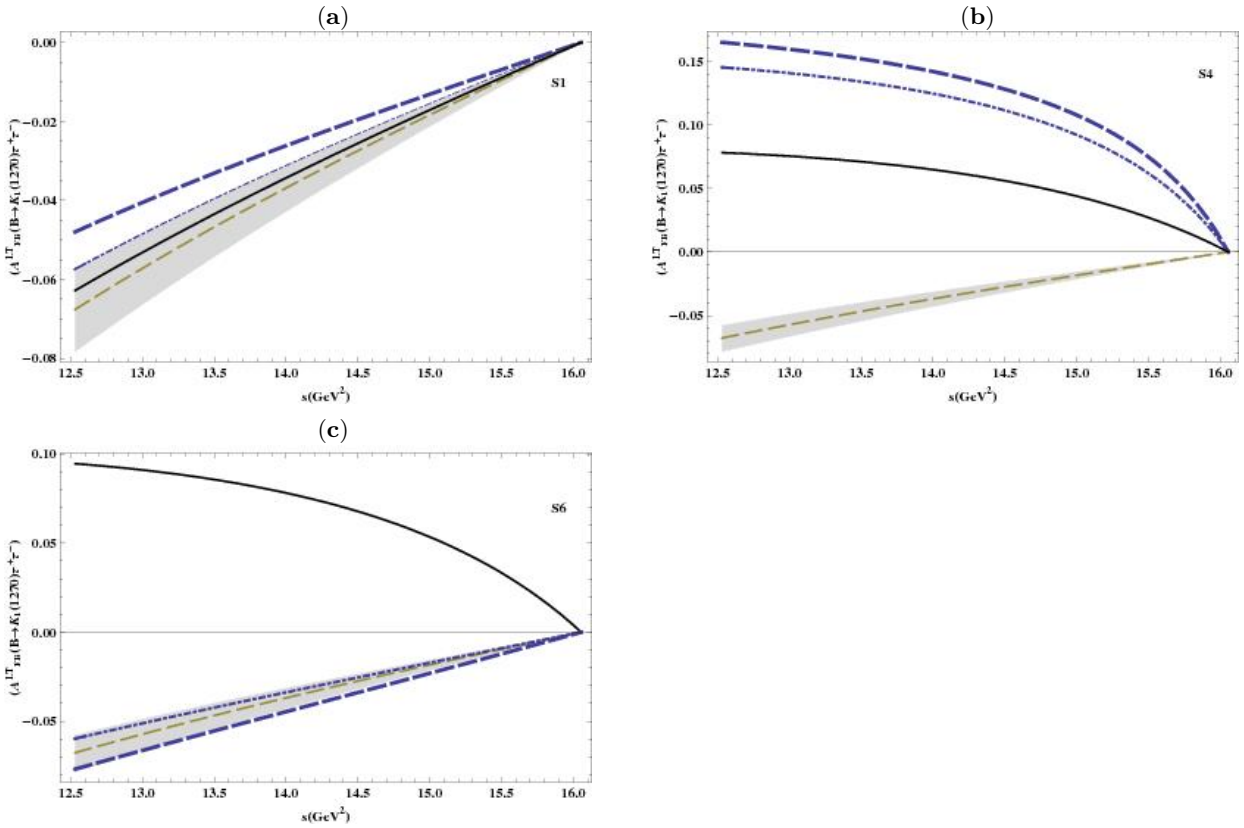

FIG. 8: The same as in figure 3, but for $B \to K_1(1270)\tau^+\tau^-$.

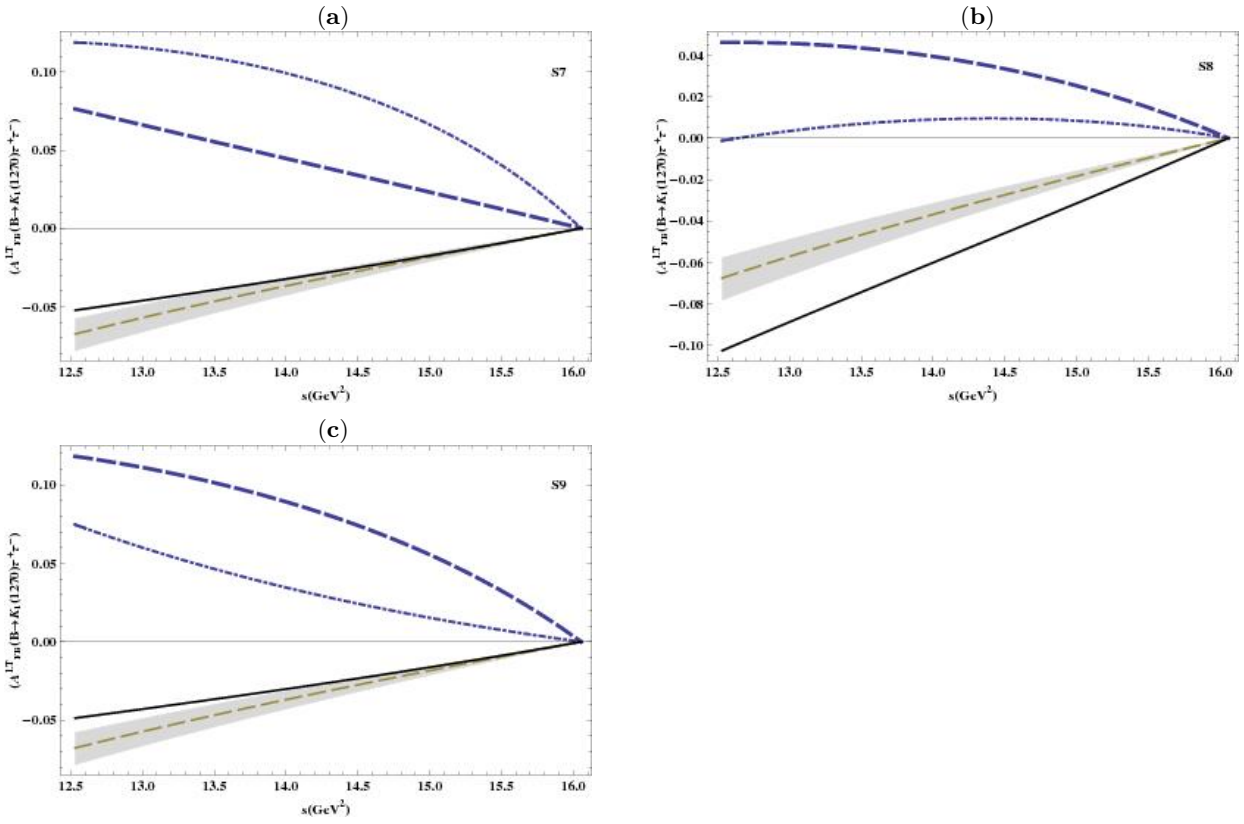

FIG. 9: The same as in figure 4, but for $B \to K_1(1270)\tau^+\tau^-$.

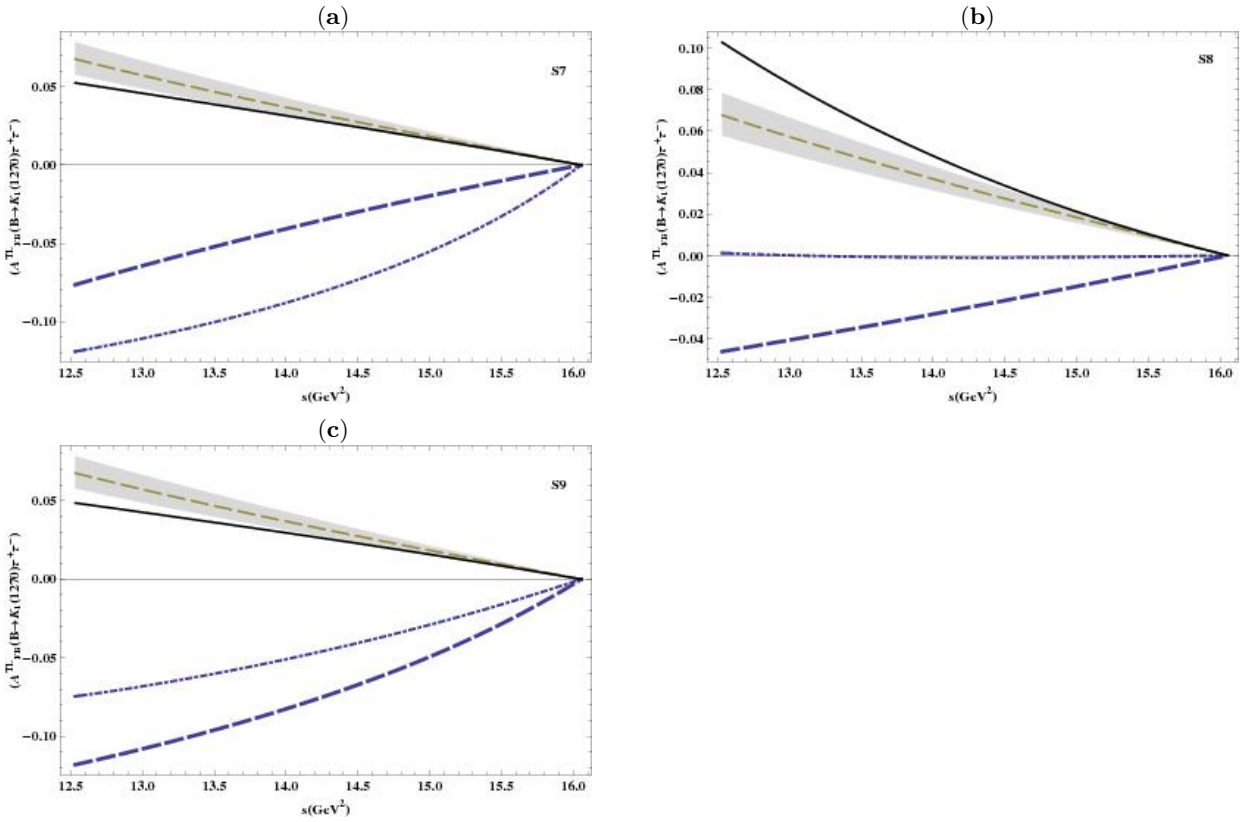

FIG. 10: The same as in figure 5, but for $B \to K_1(1270)\tau^+\tau^-$.

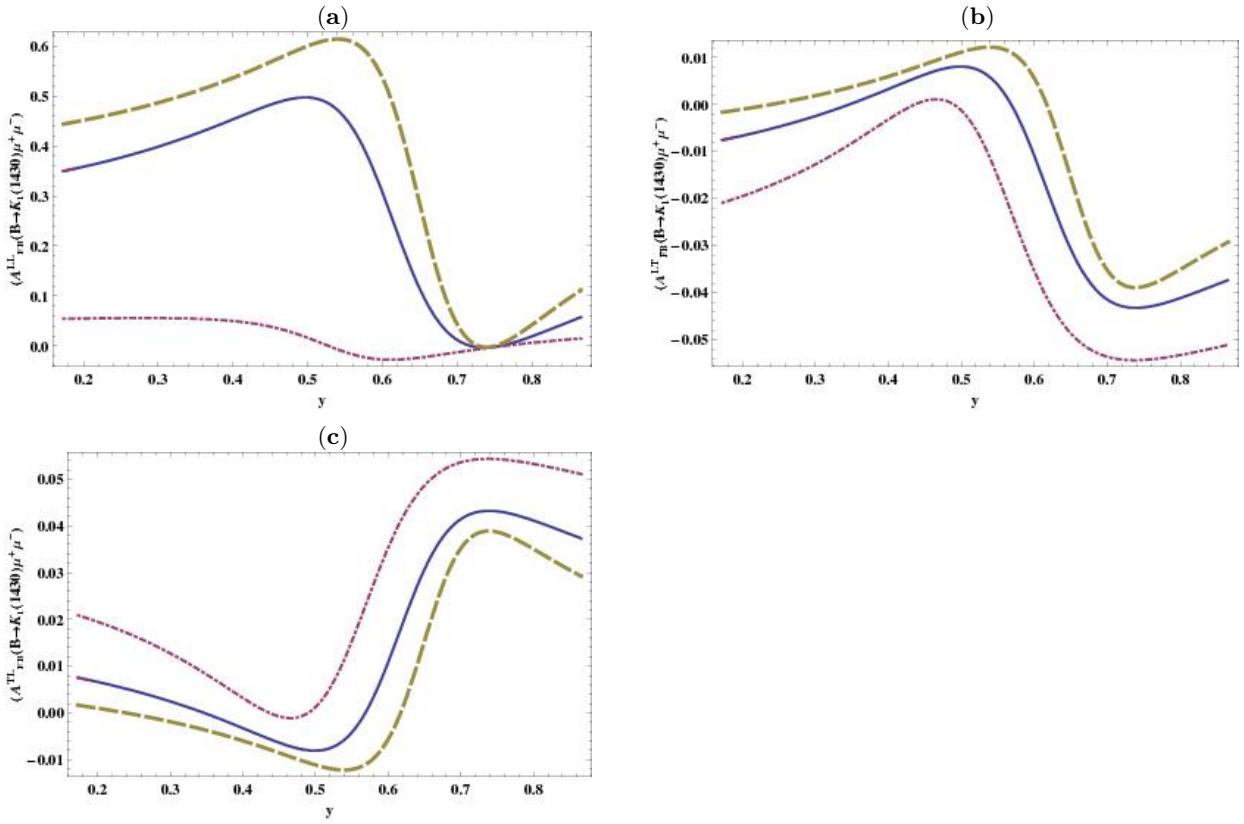

FIG. 11: Dependence of double polarized forward-backward asymmetries for the decay $B \to K_1(1430)\mu^+\mu^-$ on mixing angle θ_K, where $y = \sin\theta_K$. The dashed-dotted, solid and dashed angle dependent curves correspond to $s = 3GeV^2, 5GeV^2$ and $7GeV^2$, respectively.

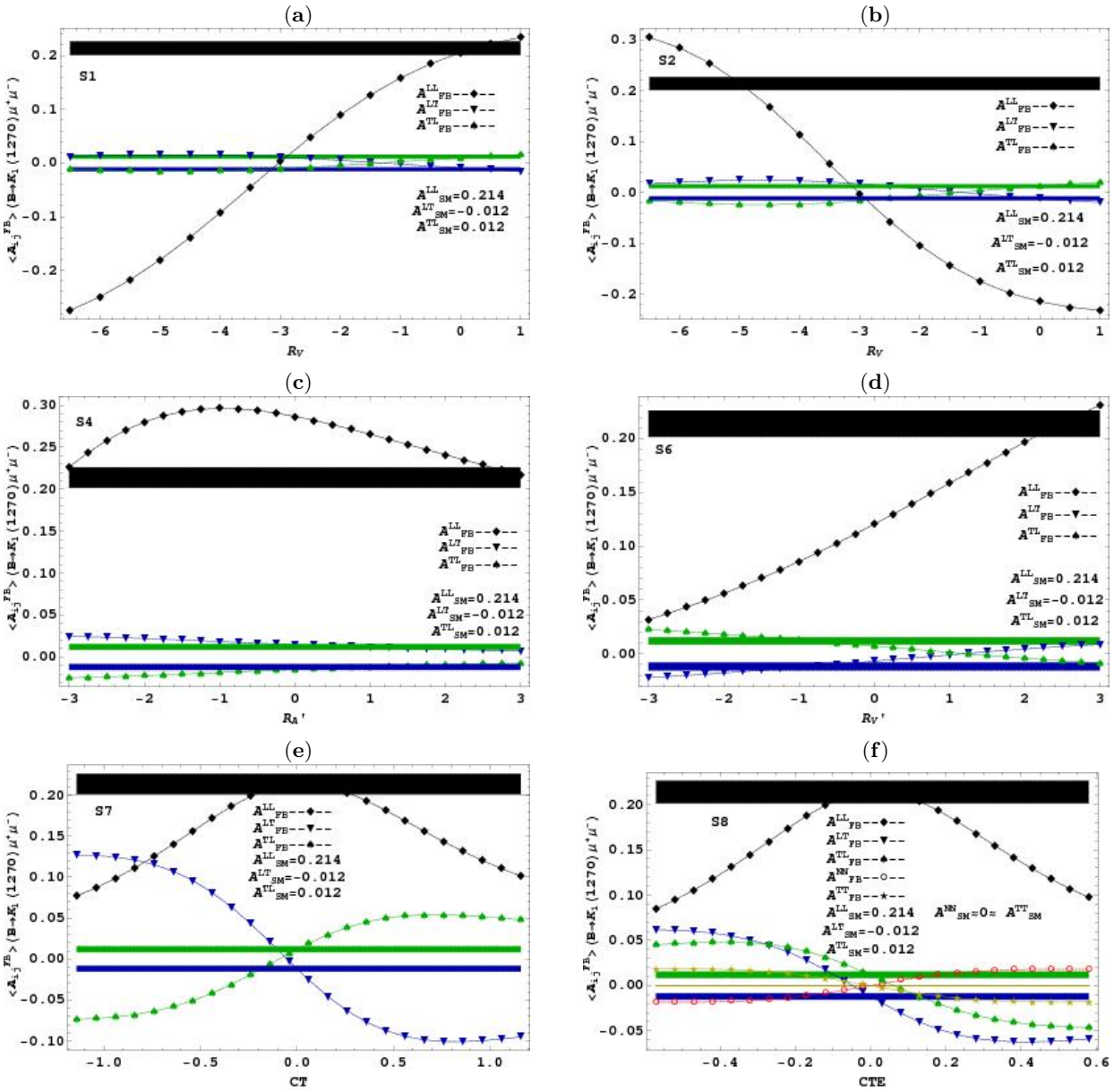

FIG. 12: Averaged double lepton Polarized forward backward asymmetries $\langle \mathcal{A}_{FB}^{ij} \rangle$ for the decay $B \to K_1(1270)\mu^+\mu^-$ in different scenarios.

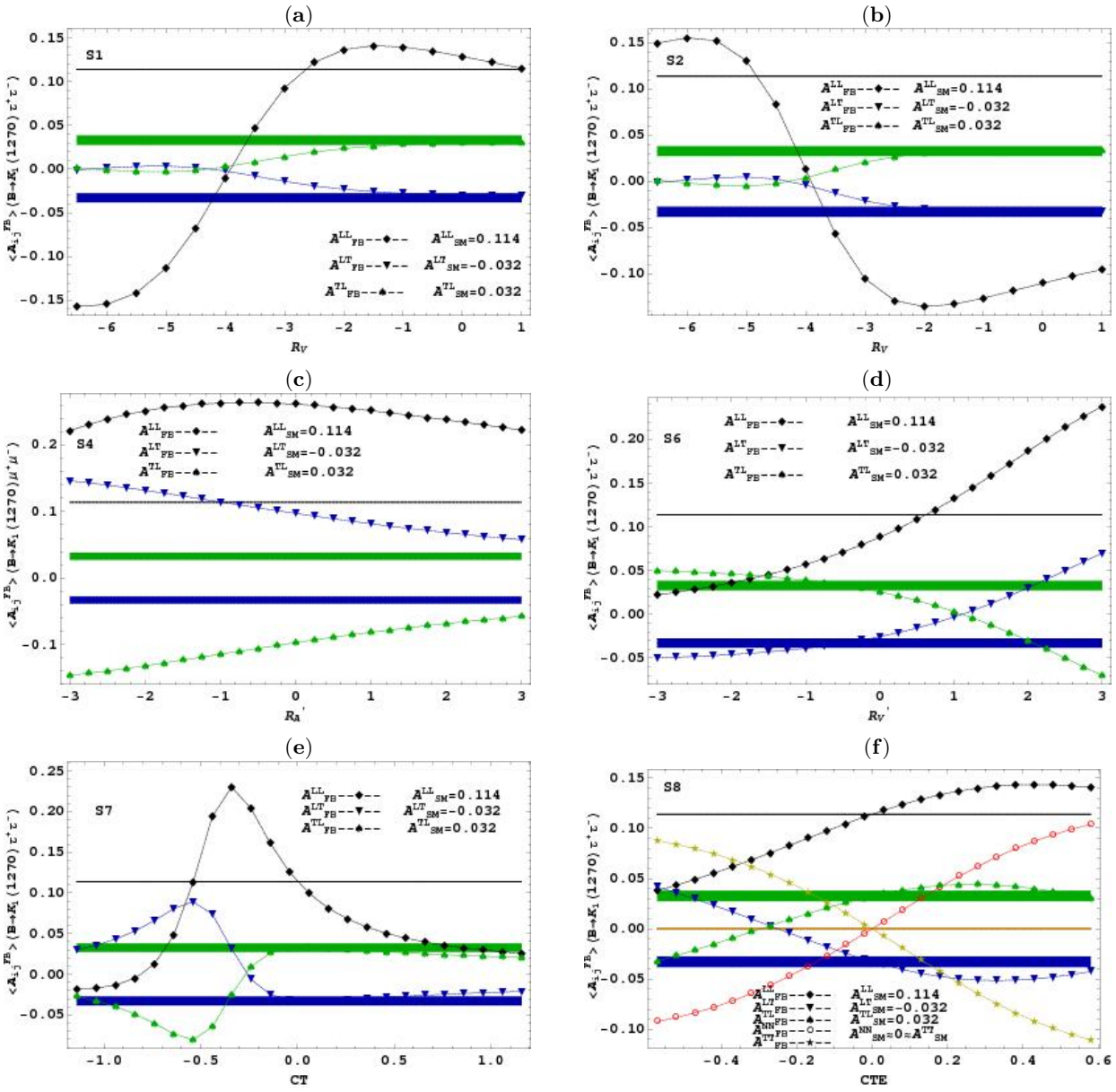

FIG. 13: Averaged double lepton Polarized forward backward asymmetries $\langle \mathcal{A}_{FB}^{ij} \rangle$ for the decay $B \to K_1(1270)\tau^+\tau^-$ in different scenarios.